

SANDIA REPORT

SAND2016-0023

Unlimited Release

Printed January 2016

Multi-Objective Advanced Inverter Controls to Dispatch the Real and Reactive Power of Many Distributed PV Systems

John Seuss, Matthew J. Reno, Matthew Lave, Robert J. Broderick, Santiago Grijalva

Prepared by
Sandia National Laboratories
Albuquerque, New Mexico 87185 and Livermore, California 94550

Sandia National Laboratories is a multi-program laboratory managed and operated by Sandia Corporation, a wholly owned subsidiary of Lockheed Martin Corporation, for the U.S. Department of Energy's National Nuclear Security Administration under contract DE-AC04-94AL85000.

Approved for public release; further dissemination unlimited.



Sandia National Laboratories

Issued by Sandia National Laboratories, operated for the United States Department of Energy by Sandia Corporation.

NOTICE: This report was prepared as an account of work sponsored by an agency of the United States Government. Neither the United States Government, nor any agency thereof, nor any of their employees, nor any of their contractors, subcontractors, or their employees, make any warranty, express or implied, or assume any legal liability or responsibility for the accuracy, completeness, or usefulness of any information, apparatus, product, or process disclosed, or represent that its use would not infringe privately owned rights. Reference herein to any specific commercial product, process, or service by trade name, trademark, manufacturer, or otherwise, does not necessarily constitute or imply its endorsement, recommendation, or favoring by the United States Government, any agency thereof, or any of their contractors or subcontractors. The views and opinions expressed herein do not necessarily state or reflect those of the United States Government, any agency thereof, or any of their contractors.

Printed in the United States of America. This report has been reproduced directly from the best available copy.

Available to DOE and DOE contractors from

U.S. Department of Energy
Office of Scientific and Technical Information
P.O. Box 62
Oak Ridge, TN 37831

Telephone: (865) 576-8401
Facsimile: (865) 576-5728
E-Mail: reports@adonis.osti.gov
Online ordering: <http://www.osti.gov/bridge>

Available to the public from

U.S. Department of Commerce
National Technical Information Service
5285 Port Royal Rd.
Springfield, VA 22161

Telephone: (800) 553-6847
Facsimile: (703) 605-6900
E-Mail: orders@ntis.fedworld.gov
Online order: <http://www.ntis.gov/help/ordermethods.asp?loc=7-4-0#online>



SAND2016-0023
Unlimited Release
Printed January 2016

Multi-Objective Advanced Inverter Controls to Dispatch the Real and Reactive Power of Many Distributed PV Systems

Matthew J. Reno, Matthew Lave, Robert J. Broderick
Photovoltaics and Distributed Systems Integration
Sandia National Laboratories
P.O. Box 5800
Albuquerque, New Mexico 87185-1033

John Seuss, Santiago Grijalva
School of Electrical and Computer Engineering
Georgia Institute of Technology
777 Atlantic Drive NW
Atlanta, GA 30332-0250

Abstract

The research presented in this report compares several real-time control strategies for the power output of a large number of PV distributed throughout a large distribution feeder circuit. Both real and reactive power controls are considered with the goal of minimizing network over-voltage violations caused by large amounts of PV generation. Several control strategies are considered under various assumptions regarding the existence and latency of a communication network. The control parameters are adjusted to maximize the effectiveness of each control. The controls are then compared based on their ability to achieve multiple objectives. These objectives include minimizing the total number of voltage violations, minimizing the total amount of PV energy curtailed or reactive power generated, and maximizing the fairness of any control action among all PV systems. The controls are simulated on the OpenDSS platform using time series load and spatially-distributed irradiance data.

CONTENTS

1. INTRODUCTION.....	11
2. CONTROL TYPES EXPLORED	13
2.1. Local Voltage-Based PV Curtailment	13
2.2. Local Voltage-Based Var Control	13
2.3. Centralized Fair Curtailment Dispatch	14
2.4. Curtailment Dispatch via PV Voltage Sensitivities	15
3. BASELINE FEEDER AND PV SIMULATION.....	17
3.1. Feeder Characteristics	17
3.2. Distributed Irradiance Profiles	19
3.3. Interfacing the Matlab Simulation with OpenDSS	21
3.4. Impact of PV with No Advanced Inverter Controls	21
4. SIMULATION OF ADVANCED INVERTER CONTROLS	25
4.1. Zero Current Injection PV Control	25
4.2. Local Voltage-Based PV Curtailment	28
4.3. Local Voltage-Based Var Control	34
4.5. Centralized Fair Curtailment Dispatch	35
One-minute Dispatch.....	35
Five-minute Dispatch	40
4.7. Curtailment Dispatch via PV Voltage Sensitivities	42
One-minute Dispatch.....	42
Five-minute Dispatch	47
5. CONCLUSIONS	51
6. REFERENCES.....	54

FIGURES

Figure 1. Volt/Watt droop curve used for local PV power curtailment.....	13
Figure 2. (left) Volt/Var control curve used for local PV reactive power support. (right) Assumed relationship between real power output and reactive power available to PV inverter.	14
Figure 3. Map of Feeder CO1 with line thickness representing current magnitude and color representing relative voltage level.	17
Figure 4. 10-minute average ANSI voltage violations in a year with no PV placed on the feeder.	18
Figure 5. Map of feeder CO1 with PV placements indicated and lines colored by per-unit voltage.....	19
Figure 6. Feeder voltage profile at minimum load without PV and with PV, represented as yellow stars.	19
Figure 7. Irradiance time offset used per load transformer in the feeder based on historical wind speeds.	20
Figure 8. Example of the time-shifted global horizontal irradiance (GHI) compared with original data (blue).....	20
Figure 9. Yearly feeder real and reactive load with and without PV (left) and a zoomed-in segment (right).	21
Figure 10. 10-minute average ANSI voltage violations in a year with PV placed at each load, sized at 150% minimum daytime load.	22
Figure 11. Percent of the feeder that is over-voltage any time during a day for one-year simulation.....	23
Figure 12. Total over-voltage violations during worst week of the year.....	23
Figure 13. Real power load and PV output at first load in feeder during worst-case week.	25
Figure 14. Substation power with and without zero-current injection control.	25
Figure 15. Power output and local load of a single PV system under ZCI control.	26
Figure 16. Percent difference in PV power output from local load consumption for a single PV system under ZCI control.....	26
Figure 17. Total PV generation over time with and without zero-current injection control.	27
Figure 18. Disparity of PV power curtailment using ZCI control during the worst week and year.	27
Figure 19. Comparison of the performance during the worst week for different local control parameter sets.....	28
Figure 20. Impact of Volt/Watt control parameters on power oscillations due to irradiance.....	29
Figure 21. Volt/Watt control parameter comparison with lowered maximum power rate of change.	29
Figure 22. Impact of Volt/Watt control parameters on PV system power output with lowered inverter maximum power rate of change.	30
Figure 23. Total PV power generation during worst week with tuned Volt/Watt control.....	31
Figure 24. Disparity of PV power curtailment using Volt/Watt control during one week and over one year.	31

Figure 25. Total curtailment of PV energy during each day in the year under Volt/Watt control.	32
Figure 26. Geographic distribution of PV system curtailment in the circuit due to Volt/Watt control.	32
Figure 27. Distribution of largest PV systems in the circuit and relative line voltages.....	33
Figure 28. Zoomed section of highest curtailment in feeder due to Volt/Watt control.	33
Figure 29. (top) PV real and reactive power output during worst week of voltage violations with Volt/Var control. (bottom) Total voltage violations seen on feeder with Volt/Var control.	34
Figure 30. All irradiance multiplier time series for worst week of voltage violations.	35
Figure 31. Comparison of the performance of an initial set of different central fair control parameter sets.	36
Figure 32. Result of increasing regulator gain from lower value (top) to higher value (bottom).	36
Figure 33. Comparison of the performance of the updated central fair control parameter sets. ..	37
Figure 34. Centralized fair curtailment control time-domain performance comparison for (top) $V_{lim}=1.049$ and (bottom) $V_{lim}=1.048$	38
Figure 35. PV power output using tuned fair dispatch control parameters during the worst week.	38
Figure 36. Disparity in PV power curtailment using fair centralized dispatch during worst week.	38
Figure 37. Percent of time feeder is in violation during each day of the year under fair curtailment.....	39
Figure 38. Percent of feeder in voltage violation during the year under fair curtailment.....	39
Figure 39. Percent of total PV system power output curtailed during each day of the year under fair curtailment.	40
Figure 40. Geographic distribution of PV system curtailments in the circuit due to fair dispatch control.	40
Figure 41. Comparison of the performance of different fairly dispatched control parameter sets under five-minute dispatch.....	41
Figure 42. Curtailment comparison of three different control parameters for fair dispatch control under 5-minute dispatch window.	41
Figure 43. Comparison of a single day of fair dispatch control operating with 5-minute dispatches under three different regulator gains.	41
Figure 44. Disparity in the amount of power curtailment seen by the PVs under fair centralized control with a five-minute dispatch window.....	42
Figure 45. Comparison of the performance of different sensitivity-based control parameter sets.	43
Figure 46. Worst week time series PV curtailment using centralized sensitivity-based PV dispatch at 1-minute intervals.	43
Figure 47. Disparity in the amount of power curtailment seen by the PVs under sensitivity-based control.	44
Figure 48. Geographic distribution of PV curtailments in the circuit due to sensitivity-based dispatch control during the worst week.	45

Figure 49. Zoomed-in section showing location of PVs curtailing the most due to sensitivity-based dispatch control during the worst week.	45
Figure 50. Geographic distribution of PV curtailments in the circuit due to sensitivity-based dispatch control over the year.	46
Figure 51. Zoomed-in section showing location of PVs curtailing more due to sensitivity-based dispatch control over the year than during worst week.....	47
Figure 52. Comparison of sensitivity-based five-minute dispatch control parameter set performance.....	47
Figure 53. PV output power with and without five-minute dispatch sensitivity-based curtailment and remaining voltage violations with control.....	48
Figure 54. Zoomed-in section of a day under five-minute dispatch of sensitivity-based curtailment.....	48
Figure 55. Disparity in PV power curtailment using sensitivity-based control dispatched at 5-minute intervals.....	49

TABLES

Table 1. Comparison of the performance of the various PV inverter control types investigated during the worst one-week period of voltage violations on the feeder.	51
Table 2. Comparison of the performance of the various PV inverter control types investigated during over full year of load and irradiance data.	51

NOMENCLATURE

ANSI	American National Standards Institute
DG	Distributed Generation
DOE	Department of Energy
IEEE	Institute of Electrical and Electronics Engineers
MW	Megawatts (AC)
OpenDSS	Open Distribution System Simulator™
PCC	Point of Common Coupling
pu	per unit
PV	Photovoltaic
QSTS	Quasi-static Time-series
ZCI	Zero Current Injection

1. INTRODUCTION

As photovoltaic (PV) generation becomes increasingly adopted on distribution networks, recent research has sought to find the physical constraints on the amount and usage of PV that existing distribution networks can handle. Some research has focused on how the amount of PV that can be installed on a network is limited by the PV's impact on network voltage and line current limits [1]. Other research investigates how the amount of PV is limited by the PV's interaction with existing network devices, such as voltage regulators and overcurrent relays [2-4]. These studies typically assume no control of the PV's grid-tie inverter since existing interconnection guidelines do not allow for any voltage regulating control by distributed generation (DG). So-called "smart inverter" controls could allow the PV inverters to provide reactive power support when available or curtail their real power output when necessary to keep the network within operational constraints. Utilities, especially those in states with high renewable portfolio standards, are therefore very interested in implementing smart inverter controls on PV systems interconnected to their networks if the controls can be proven to be safe and effective [5].

Recent research has shown that the addition of passive voltage monitoring local controls to PV inverter can mitigate many of the adverse effects caused by distributed PV systems [6-9]. Improved functionality may be possible if some level of communication exists between the inverters [10, 11]. In particular, many researchers look to find the optimal dispatch of PV inverter reactive power in the presence of a communication network [12-15]. The problem can be further extended to the optimal dispatch of both real and reactive power [16, 17]. Ideally, control of PV inverters should be coordinated with existing voltage regulators to achieve the best results [18, 19]. In these studies, the dynamics of the inverters are assumed to be locally stable and thus only require a power reference to be solved for at a particular load and irradiance level. Therefore, these simulations use quasi-static time-series (QSTS) data of load and irradiance to study controller performance over time. Still, optimal power dispatch approaches are typically computationally intensive and only study short time periods. Local control approaches are more easily studied over large time series, but the tuning of their control parameters that yield the best results is not straightforward [20]. A comparison between the performances of local versus centralized control strategies over long time periods is therefore complicated by the vast difference in simulation times. This problem is only further complicated by the complexity of the distribution network studied and the number of PV controlled.

This paper focuses on the application of smart inverter controls to a large number of highly distributed PV systems in a realistic distribution network. To effectively study the time-dependent and unpredictable nature of PV, a full year of irradiance and load data is studied. The goal of this research is to study how smart inverter controls can be used to mitigate the rise in network voltage caused by a large amount of PV distributed throughout a distribution feeder. The details of the simulated system is described in Chapter 3, but a sufficient amount of PV generation is placed on the network to ensure over-voltage is a legitimate problem during daytime periods throughout the year. Several PV inverter control strategies are compared that will either curtail the real power output or provide reactive power support based on network conditions. The goal of each control strategy is to mitigate all over-voltage violations caused by PV. Both controls that only utilize local measurements and those that require a robust communication network are tested. The details of the control strategies investigated are

presented in Chapter 2. If applicable, each controller has its parameters adjusted over a sample time period so that the controls are fairly compared. In addition to their ability to mitigate over-voltages, the controls are compared based on the amount of control action used, either power curtailed or vars produced, and the fairness of how the control action is applied across the population of PVs in the network. The simulations of each control type are presented in Chapter 4. The results are then compared and conclusions discussed along with future research directions in Chapter 5.

2. CONTROL TYPES EXPLORED

2.1. Local Voltage-Based PV Curtailment

Using only locally available measurements, the output of each PV system can be curtailed based on the point of common coupling (PCC) voltage of its respective phase. To maintain smooth control operations, the curtailment is typically performed as a ramping down of active power output beginning at some measured voltage, v_1 , as shown below in Figure 1. If voltage continues to rise, the inverter will continue to ramp down its output until it is completely curtailed at measured voltage v_2 . This type of control curve is called a “Volt/Watt droop”. The theory behind this control is similar to the “frequency droop” curve applied to automatic governor control whereby the speed of a generator is proportional to frequency rise, thus setting generator speed inversely proportional to change in frequency will result in a new stable operating point. Here, change in PCC voltage is close to being linearly proportional to PV power output, so if all PV apply this control, a new stable operating point should be present. However, the slight nonlinearity of the relation between PCC voltage and PV power output makes it difficult to precisely determine the voltages v_1 and v_2 that define the curve. For this reason, these parameters will be tuned experimentally to find the curve that best mitigates over-voltages. To ensure the control begins to curtail its power output at v_1 , the $P_{set,pu}$ axis in Figure 1 is normalized to the real power available to the PV at that point in time, not the constant rating of the panels.

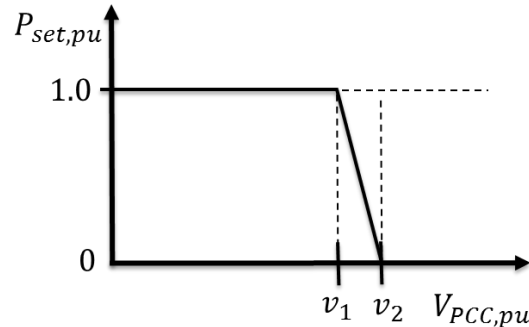


Figure 1. Volt/Watt droop curve used for local PV power curtailment.

2.2. Local Voltage-Based Var Control

A PV grid-tie inverter can supply reactive power to the grid to help regulate the line voltage by phase shifting the current it injects with respect to the voltage at its PCC. However, the capability for the inverter to provide vars is limited by its rating. In this work, it is assumed that the inverter is rated equivalent to the maximum power point its PV panels are capable of achieving, P_{MPP} . Neglecting non-idealities, the amount of reactive power available to the inverter is represented by the diagram in the right of Figure 2. Here, the radius of the circle represents the rating of the inverter and the red dashed lines indicate the range of reactive power capability for the hypothetical level of PV output power shown. The reduced power level can either be due to the PVs panels operating below P_{MPP} due to lack of rated incident irradiance or due to active

curtailment from a control, such as Volt/Watt. PV panels are seldom operating at P_{MPP} , so there is typically some reactive power available to the inverter.

The var limits from the right of Figure 2 determine the per-unit scale of the Volt/Var curve shown on the left in Figure 2, which dictates how the inverter outputs its available reactive power based on the voltage measured at the PCC. Again, this means the $Q_{set,pu}$ axis in Figure 2 is normalized to the amount of reactive power available at each point in time, not the inverter's rating. Similar to Volt/Watt, a negative droop curve is employed to supply the proper vars that will regulate the PCC voltage towards its nominal value. A deadband is used to prevent oscillation around the nominal network voltage. The curve is thus defined by the four points along the voltage axis that determine where the output will saturate and where the deadband exists, $\mathbf{x} = [x_1 \ x_2 \ x_3 \ x_4]$.

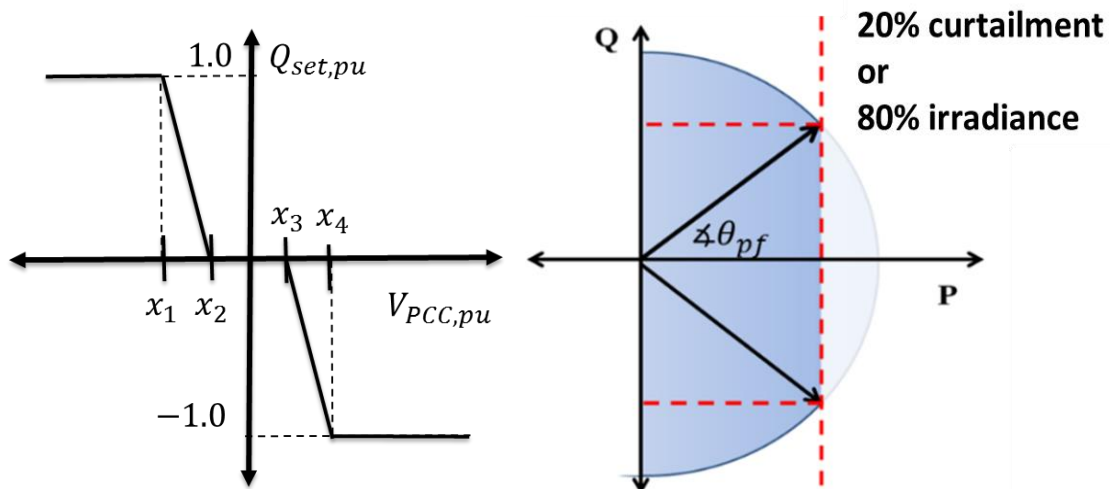


Figure 2. (left) Volt/Var control curve used for local PV reactive power support. (right) Assumed relationship between real power output and reactive power available to PV inverter.

2.3. Centralized Fair Curtailment Dispatch

The previous two control methods have assumed that no communication network exists to assist in controlling the PV inverters, so they must rely on local measurements only. If the PV inverters are able to communicate with a centralized controller, this controller would then have knowledge of all network voltages and could strategically dispatch control signals to the specific inverters that would be best suited to mitigate over-voltage violations. However, simply controlling the inverters that will mitigate over-voltages first may unfairly target a few PV installations on the network. With a centralized approach, knowledge of each inverter in the network means that fairness of the control can also be taken into consideration in the control algorithm itself.

The first centralized method is investigated to see how well inverters can mitigate over-voltages by curtailing them all an equal proportion at each time step. To this end, a regulator is established that determines the percent each PV should curtail from its available power at time instant k based on the deviation of the maximum voltage in the network from a desired voltage limit, V_{lim} .

$$\alpha(k+1) = K_{\Phi}\alpha(k) + K_R(\max(V_i(k)) - V_{lim}) \quad (1)$$

The curtailment ratio α in (1) is dispatched to each inverter at each discrete time step, k . An inertia gain, K_{Φ} , can be adjusted to weight the importance of the past step. The speed of this regulator can be set by the gain K_R , which must be tuned depending on the rate at which the signal is dispatched to the PV. Since this is a discrete controller with physical constraints, there is an upper limit to K_R beyond which the control will oscillate between saturated states. This upper limit is proportional to the rate at which the control updates and the rate at which the inverters respond. When inverter i receives the curtailment ratio α , it sets their power reference signal as a function its maximum power point (MPP) power and the local irradiance at that time step $I_i(k)$.

$$\begin{aligned} P_i(k) &= \alpha(k)P_{i,max}(k) \\ P_{i,max}(k) &= I_i(k)P_{MPP,i} \end{aligned} \quad (2)$$

2.4. Curtailment Dispatch via PV Voltage Sensitivities

This approach takes into consideration the linear approximation of voltage change in the network due to curtailment of each individual PV system. The first-order approximation assumes the change in network voltage can be found via (3).

$$\Delta V = A\Delta P + B\Delta Q \quad (3)$$

The matrices A and B are the so-called sensitivity matrices that relate change in PV system real power output ΔP and reactive power output ΔQ to change in network voltage. There are several approaches to finding the sensitivity matrices for a given distribution of PVs in a network. One method is to take a first-order linearization of the system equations. If the network equations are of the form $f(V, P, Q) = 0$, then the sensitivity matrices would be the Jacobian related to each PV input:

$$\begin{aligned} A &= \frac{\partial V}{\partial P} \\ B &= \frac{\partial V}{\partial Q} \end{aligned} \quad (4)$$

However, it is difficult to easily formulate the network equations in this form for an unbalanced, three-phase system. Often, power flow software does not expose these sensitivities to the user and a practical approach is to utilize the power-flow solution to obtain the change in network voltages due to curtailment of PV systems directly. For this procedure, each PV system j has its output power curtailed by a percentage of its per-unit rating, Δp , such that $P_j = P_{j0} - \Delta p$. The columns of the real power sensitivity matrix can then be populated with the resulting difference in voltage from the zero-curtailment case, V_0 . The reactive power sensitivity matrix can be found similarly by adjusting the output of each PV system up by some Δq once curtailed.

$$\begin{aligned} \mathbf{A} &= [\mathbf{a}_1 \ \mathbf{a}_2 \ \dots \ \mathbf{a}_j \ \dots \ \mathbf{a}_n] \\ \mathbf{a}_j &= \mathbf{V}_j - \mathbf{V}_0 \end{aligned} \quad (5)$$

The optimum (minimum) amount of power curtailment that mitigates all over-voltages for the measured system state \mathbf{V} is then the solution to the following linear programming problem:

$$\begin{aligned} \min_{\Delta P_j} \quad & \sum_{j=1}^n \Delta P_j \\ \text{s. t.} \quad & \begin{cases} \mathbf{A}\Delta\mathbf{P} \leq 1.05 - \mathbf{V} \\ \mathbf{p}_{min} \leq \Delta\mathbf{P} \leq \mathbf{p}_{max} \end{cases} \end{aligned} \quad (6)$$

The first line in (6) assures that the curtailment is minimized, the second line assures that the curtailments bring the over-voltage values within the nominal voltage range, and the last line assures the curtailment values are valid. Due to the last line, the state of curtailment must be recorded and passed between dispatch solutions. Additionally, there is no guarantee for any given system state \mathbf{V} that there exists a change in PV system power outputs, $\Delta\mathbf{P}$, that satisfies the constraints, even if all PVs are curtailed. This may seem counter-intuitive at first if the network over-voltages are caused by the PV real power injection and should therefore be fully mitigated if the PV are fully curtailed. However, this optimization does not take into consideration the state of the voltage regulators since in this work it is assumed that they can neither be measured nor controlled. Without taking the regulator controls into consideration, the dispatch solution provided by (6) will tend to oscillate. Under these restrictions, an optimization of (6) cannot provide the inverter power dispatches, so another approach must be taken.

To account for the action of the voltage regulators, a smoothing approach is developed by integrating the desired curtailment of all inverters, $\Delta\mathbf{P}$, at each time step within their physical limits. Thus, the curtailment of each inverter, ΔP_j , becomes a state variable to be updated and passed between time steps and then dispatched to the PV at the appropriate interval. The time step k represents either 1-minute or 5-minute dispatch to the PV in the later simulations. The curtailment vector is updated by the inverse sensitivity matrix times the desired change in voltage and a tunable gain K_A , as shown below in (7).

$$\begin{aligned} \Delta\mathbf{P}(k+1) &= \Delta\mathbf{P}(k) + K_A \mathbf{A}^{-1}(\mathbf{V}(k) - \mathbf{V}^*) \\ \text{s. t.} \quad & (-1 \leq \Delta\mathbf{P}(k) \leq 0) \\ & |\Delta\mathbf{P}(k+1) - \Delta\mathbf{P}(k)| \leq \Delta P_{lim} \end{aligned} \quad (7)$$

The inequality constraints in (7) are added to keep the control actions bounded to physical constraints. The 2nd line in (7) represents the fact that an inverter cannot curtail or produce more power than that flowing through it. To prevent oscillations between controllers, the amount each PV can ramp between iterations is limited to 20% of its rated power per minute, which is achieved by setting $\Delta P_{lim} = 0.2$ in the 3rd line of (7). The desired voltage to regulate to in (7), \mathbf{V}^* , is initially set to the ANSI limit of 1.05, however, this value can be reduced to account for inaccuracies of the linear approximation and mitigate any remaining voltage violations. In addition to \mathbf{V}^* , the control in (7) can be tuned by the gain variable K_A and the curtailment change limiter ΔP_{lim} .

3. BASELINE FEEDER AND PV SIMULATION

3.1. Feeder Characteristics

A real distribution feeder is modeled in OpenDSS to test the PV controls. The circuit, designated Feeder CO1, is a rural 12kV distribution feeder consisting of 2970 medium- and low-voltage buses and 2569 lines servicing 1447 loads through 401 service transformers. A map showing the layout of the feeder topology and the existing voltage regulating devices is shown in Figure 3. The furthest bus is 21.4km from the substation. There is one three-phase voltage regulator on the feeder backbone about 6km from the substation and five switching capacitors. The coloring of the lines in Figure 3 represents the relative line voltages and demonstrates how voltage drops with distance from the substation and voltage regulator. The line thickness represents the current flow in the lines. These plots were created with the GridPV Matlab toolbox [21],[22]. The feeder has a peak load of 6.41MW and operates at a native power factor of 0.917 at peak load. The minimum load within the year of data simulated is 20.1% of the peak load, or 1.29MW. To simulate the variation in load over the course of the year, the average of the three substation SCADA phase current measurements is taken and then normalized to create a multiplier time series that varies between [0.201, 1.0]. The reason the average of the three phases is used is because the correct phasing of the loads and measurements could not be verified. This time series has one-minute resolution and is allocated to all loads in the network since only the substation aggregate measurements are available. The loads remain at their individual constant power factors during the simulation.

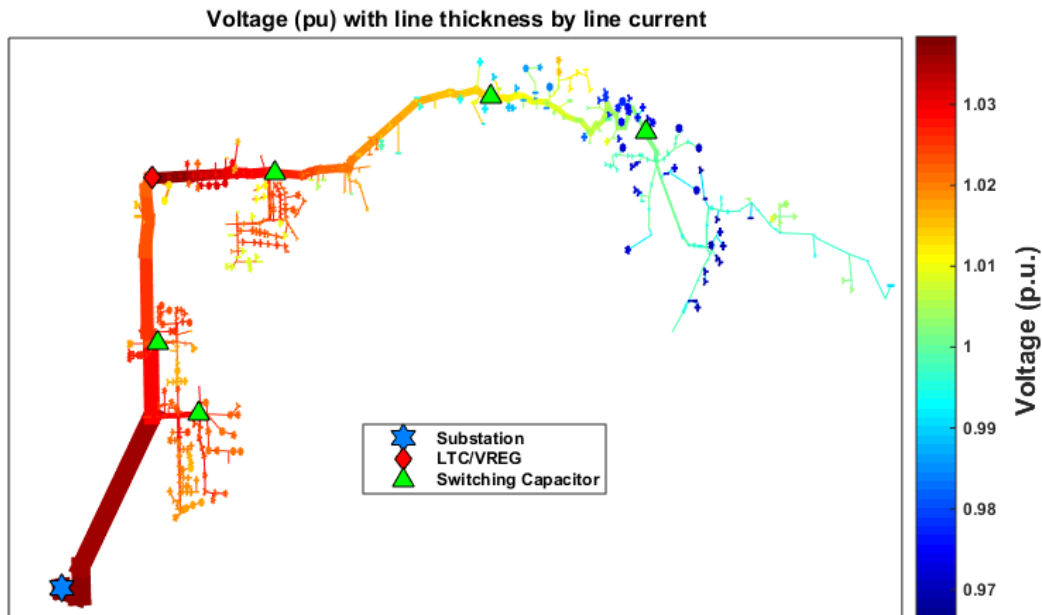


Figure 3. Map of Feeder CO1 with line thickness representing current magnitude and color representing relative voltage level.

The baseline voltage profile of the feeder simulated over the course of a year without any PV results in numerous under-voltage violations, as depicted in Figure 4. In this figure, the amount of time each load phase in the feeder spends in a voltage violation is shown. A bus is in violation

if its voltage is outside the ANSI Range-A $0.95 \leq V_{pu} \leq 1.05$ limits on a moving 10-minute average. Over-voltage violations are shown in the top plot and rarely occur without PV. The node number roughly corresponds to increasing distance down the feeder. Under-voltage violations are shown in the bottom plot and occur at numerous loads, especially towards the end of the feeder. The nodes with the most under-voltage violations are only in violation roughly 3% of the year. However, since adding PV to the network will only improve the under-voltage conditions of the network, unless the voltage regulator has load drop compensation [23], from this point on only over-voltage violations will be considered as a goal for improvement by the control of the PV inverters.

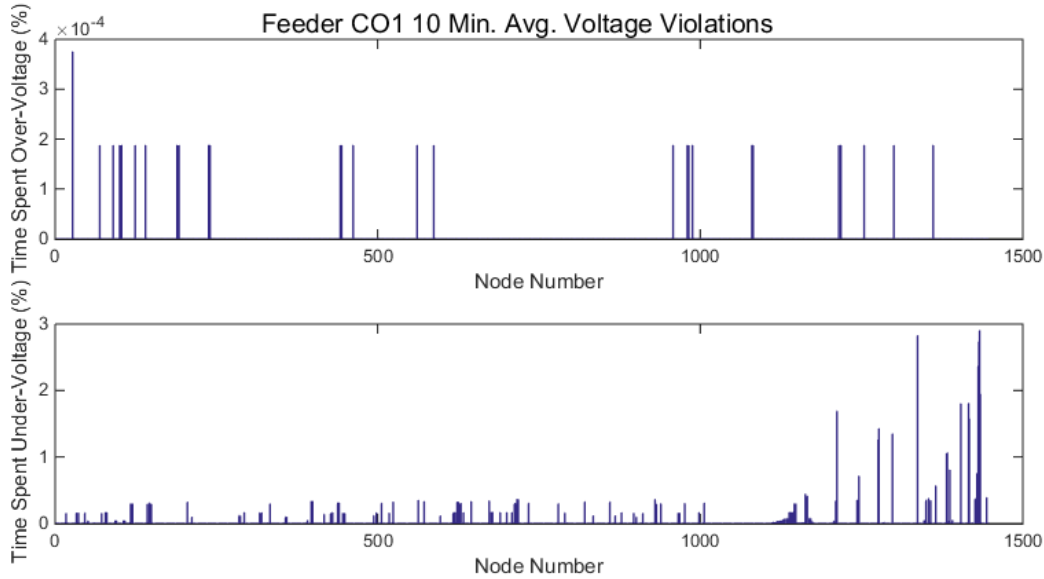


Figure 4. 10-minute average ANSI voltage violations in a year with no PV placed on the feeder.

In total, 2079 single-phase PV systems are placed on the feeder, one at each load, as shown in Figure 5. The lines in this figure are color-coded by the voltage level, which is not in violation for the snapshot of load and irradiance shown here. Each PV system is sized to represent 60% of the peak value of the local load to which it is connected. This is equivalent to 250% of the minimum daytime load within the year, which means there will be reverse power flows and voltage rise. The average per-phase PV system is 1.74kW at its peak power, P_{MPP} , which occurs at irradiance equal to $1000W/m^2$. The rated output of all PVs in the network is 3.62MW.

The voltage profile plots in Figure 6 demonstrate the voltage-rise effect of the PV during a period of low load and high irradiance. The bottom three lines without yellow stars are the voltage profiles of the three feeder phases without PV at this load level. The top three lines are the same load level with PV added at the locations indicated with a yellow star. The fact that voltage rises with distance from the substation rather than sagging is an indication that the PVs are reversing current through the lines. Since PV is installed proportionally at each load, this means that the PV are back-feeding the substation in this figure. The next section will discuss how the PV systems behave during the time-series simulation.

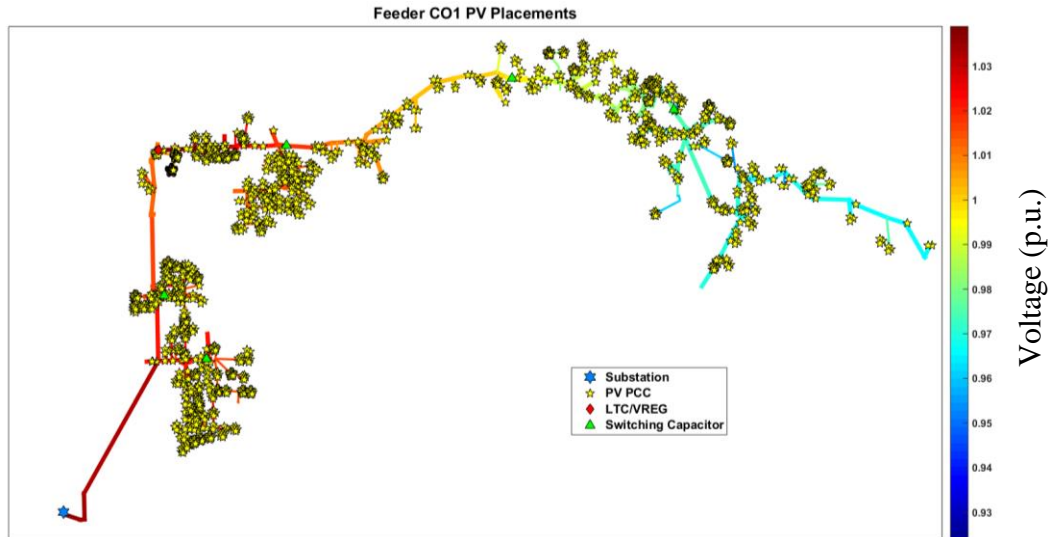


Figure 5. Map of feeder CO1 with PV placements indicated and lines colored by per-unit voltage.

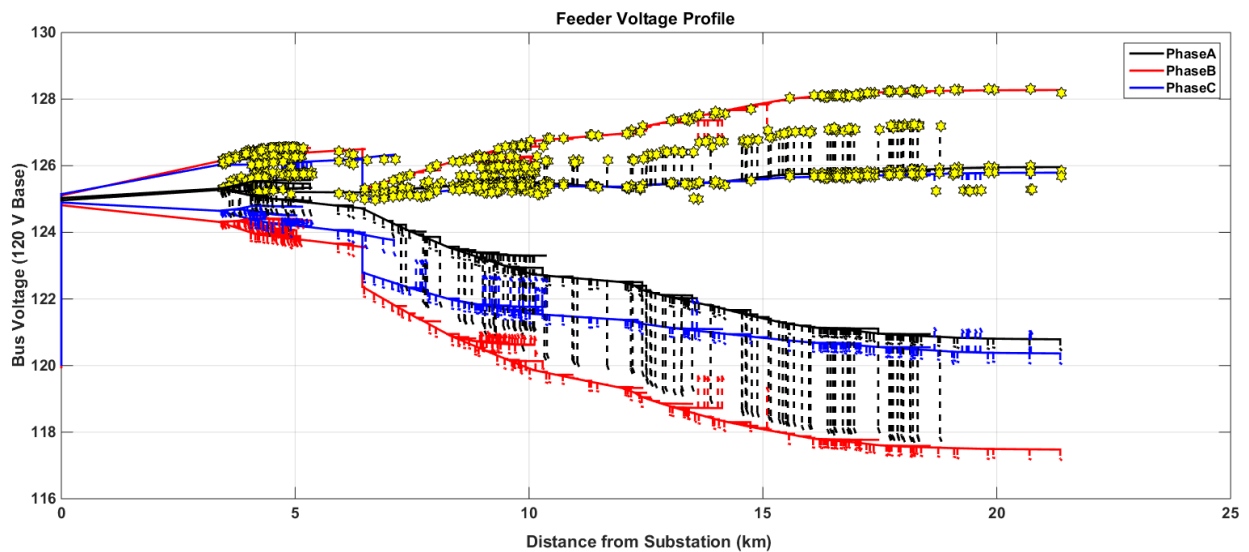


Figure 6. Feeder voltage profile at minimum load without PV and with PV, represented as yellow stars.

3.2. Distributed Irradiance Profiles

To properly investigate the interaction between the controls of multiple PV systems, they cannot be given the exact same input irradiance signal. In practice, moving clouds cause PV systems to have different amounts of available power from their neighbors. To simulate this transient effect, an irradiance profile for the entire year was created that was time-shifted based on the velocity of the clouds and the spacing of the PV installations. To achieve this, historical daily cloud speeds were matched to the irradiance data and clouds were assumed to move west to east across the feeder. Then, a time offset of cloud-arrival times was calculated for each load transformer. Figure 7 shows the time offsets for each transformer for a cloud speed of 11.4m/s. To create simulated irradiance time series for each transformer, 1-year of global horizontal irradiance

(GHI) measured in Albuquerque, NM was time-shifted by the appropriate time offset, as seen in Figure 8, which shows the simulated GHI for a transformer with a 7 minute time offset. The GHI measurements were translated to plane of array irradiance for south-facing fixed-latitude-tilt PV systems. To convert this simulated irradiance to PV DC power available to inverters, DC derates of 6% due to soiling, wiring, and mismatch losses were assumed.

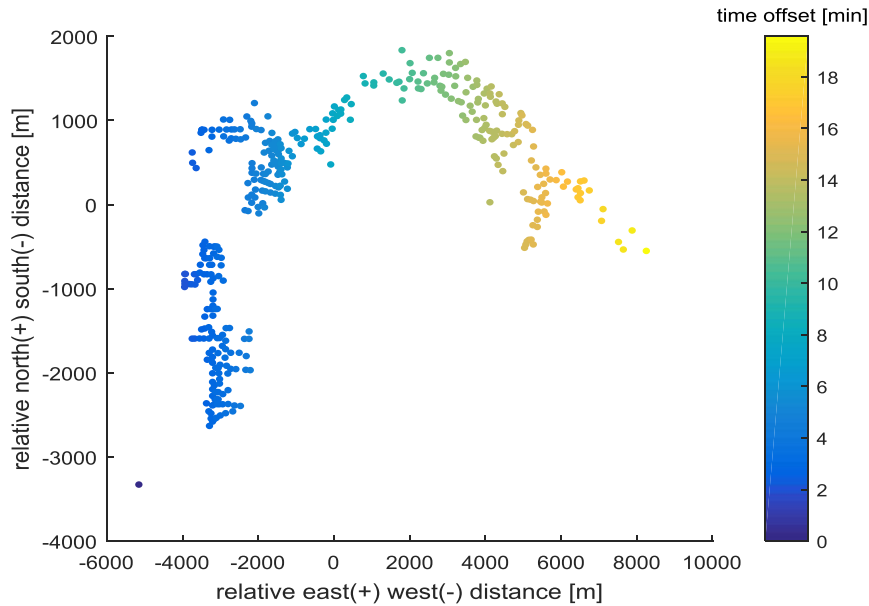


Figure 7. Irradiance time offset used per load transformer in the feeder based on historical wind speeds.

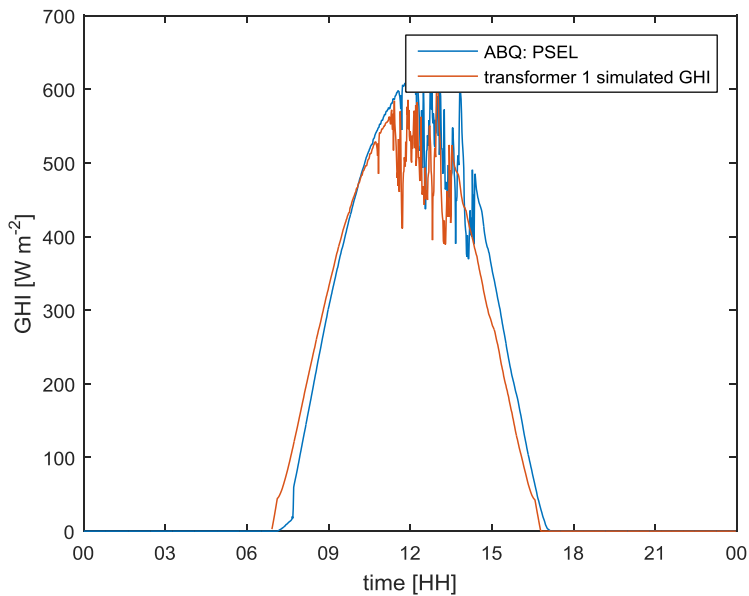


Figure 8. Example of the time-shifted global horizontal irradiance (GHI) compared with original data (blue).

3.3. Interfacing the Matlab Simulation with OpenDSS

This section will briefly describe how the simulation and controls are run in the Matlab and OpenDSS platforms. The simulation is run in a Matlab script that stores parameters, performs some control actions, and inputs and compiles results. The Matlab script interfaces with OpenDSS through a COM interface to run power flow solutions. The feeder model is loaded into OpenDSS and Matlab tells OpenDSS where to place PV systems and how to control their inverters. It is preferable to use OpenDSS's built-in inverter controls as they perform iterations faster. Both Volt/Watt and Volt/Var controls are implemented with OpenDSS's built-in controls. The ZCI control and both centralized approaches are performed in Matlab. For these controls, at each time step Matlab receives the network voltages and powers and based on the control type determines the power output of each PV system. It then directly edits the PV systems in OpenDSS through the COM interface to reflect the control actions and solves the next time step. Since the simulation is a time-series, the ZCI method predicts what the current time-step control should be and the centralized methods use continuous curtailment states updated by the previous solution.

3.4. Impact of PV with No Advanced Inverter Controls

The feeder is simulated with the year of spatially dispersed irradiance profiles applied to the appropriate PV system. The yearly real and reactive power demand for the feeder are shown in Figure 9 both in the baseline case without PV and with PV systems. This results in a total of 6.76GWh of power generated by PV throughout the year, an average of 3.25MWh per PV. There is much overlap in the plot due to the diurnal nature of the PV generation, so to get a sense of how much the PV impacts the base load, a zoomed-in segment around the yearly minimum load is also provided. It can be seen in the zoomed-in segment that there are times when the PV systems reverse current and begin injecting power into the transmission system.

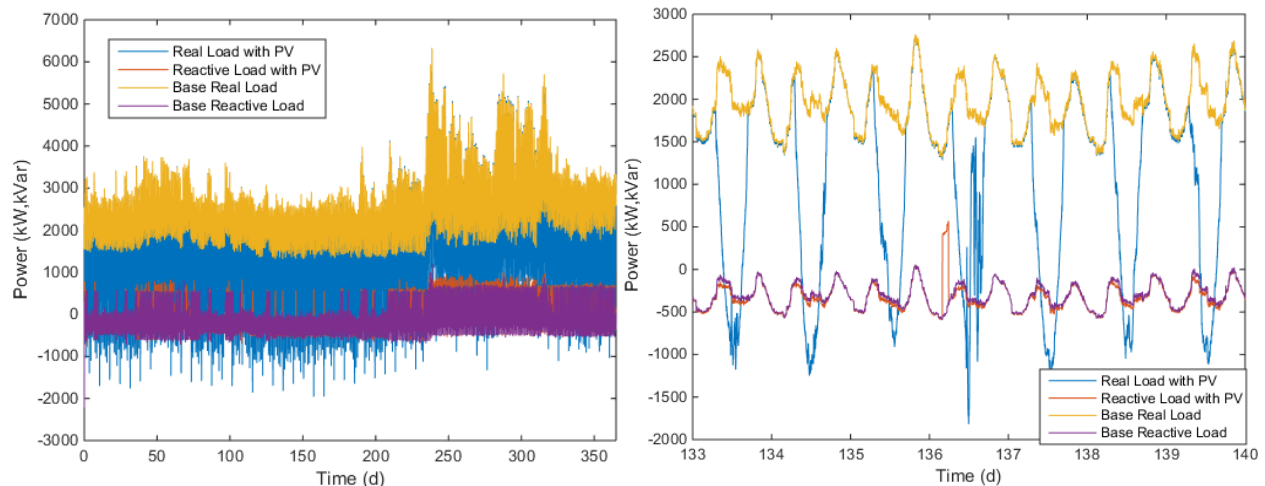


Figure 9. Yearly feeder real and reactive load with and without PV (left) and a zoomed-in segment (right).

The 10-minute average voltage violations due to this amount of PV are shown in Figure 10. As expected, the under-voltage violations are largely mitigated due to the voltage rise caused by the

PV. However, this results in a large amount of over-voltage violations, now with 4,784,242 one-minute violation periods in total across the feeder. Considering the feeder in violation if *any* bus has an over-voltage violation, then the feeder is over-voltage 18,861 minutes of the year, or 3.59% of the year. The bus with the single most violations is over-voltage 2.74% of the year. These violations are relatively uniformly distributed throughout the feeder, perhaps depending more on PV system size than location.

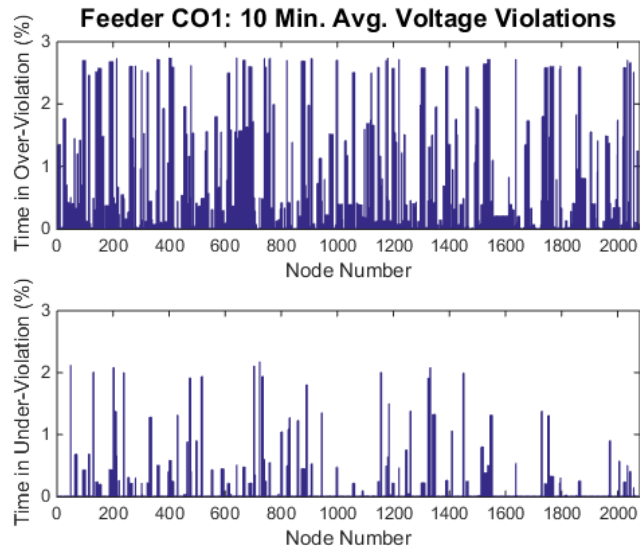


Figure 10. 10-minute average ANSI voltage violations in a year with PV placed at each load, sized at 150% minimum daytime load.

Each of the above 1-year simulations at 1-minute resolution takes slightly less than 1-hour to run on a typical 2015 desktop computer. However, once more advanced smart inverter controls are implemented on each inverter, this simulation time becomes many times larger. Additionally, the appropriate controller parameters are not known. Thus, a subset of the load and irradiance profiles is tested before running the entire year simulation. The one-week period with the single highest number of over-voltage violations in the no-control case is found. Of all the over-voltage violations that occur during the year, most occur just before the middle of the year when the load is relatively low and irradiance values are increasing, as shown in Figure 11. The worst week for over-voltage violations starts on the 132nd day of the year and accrues 433,821 minutes of violations across the feeder.

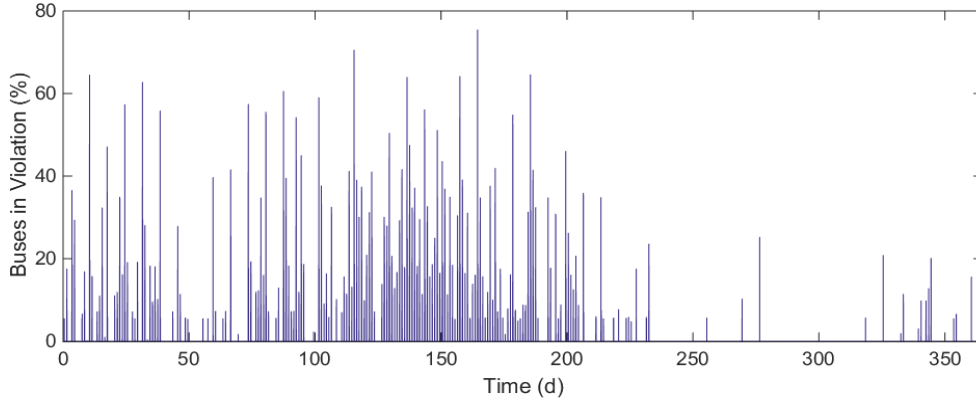


Figure 11. Percent of the feeder that is over-voltage any time during a day for one-year simulation.

Simulating this single week, as shown in Figure 12, disregards the state of the network leading up to it which slightly skews the results. Due to this there are slightly fewer violations, 413,015 in total. However, this corresponds to the feeder being in violation 13.3% of the time during this week, much greater than the entire year. Also, when eliminating nighttime (59.1% of the sample week), the feeder has a voltage violation 32.5% of the time. Tuning the local inverter controls to improve this single week should approximate the times of best improvement seen over the entire year. Without curtailment, 7.77GWh are generated during this week from the distributed PV. When tuning the controls, the goal will be to mitigate all voltage violations while minimizing the deviation from this level of PV generation.

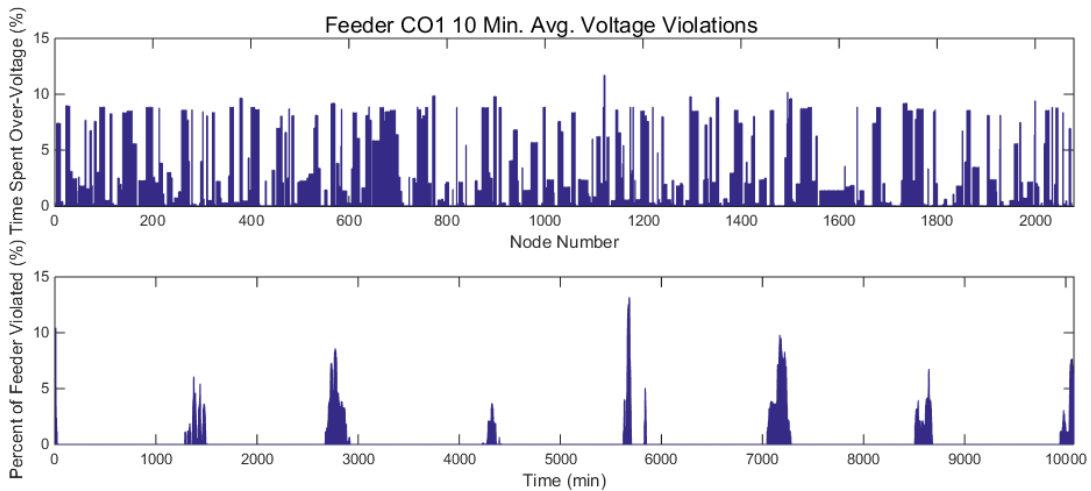


Figure 12. Total over-voltage violations during worst week of the year.

4. SIMULATION OF ADVANCED INVERTER CONTROLS

4.1. Zero Current Injection PV Control

The first curtailment control strategy investigated is to simply limit the production of the PV to not exceed that of the local load, termed zero current injection (ZCI). The theory behind this approach is that so long as the PV systems do not inject current into the distribution network, there will be no voltage rise. Thus, the inverters are controlled to match, but not exceed, the power consumption of their local load so that the PCC never sees reverse current flow. However, this curtailment strategy can significantly reduce the amount of overall renewable energy produced. Additionally, this is not a standard smart inverter control being proposed for PV inverters as they do not typically have a means of measuring local load. Figure 13 shows the real power local load and the baseline PV generation during worst-case week for over-voltages for a single PV system in the network. During the peak sunlight hours of each day, the PV system outputs more than the local load consumes and should be curtailed under this control strategy. This control action can be seen clearly in Figure 14, which shows the total real power flow through the feeder breaker both with and without the ZCI control active. In the baseline case, there is negative power flow through the breaker each day, yet with the control active, the reverse power flow is prevented.

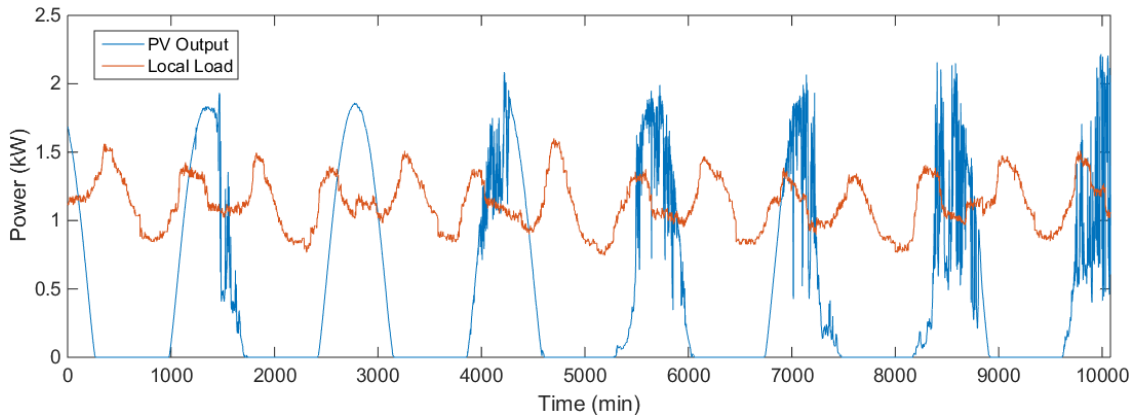


Figure 13. Real power load and PV output at first load in feeder during worst-case week.

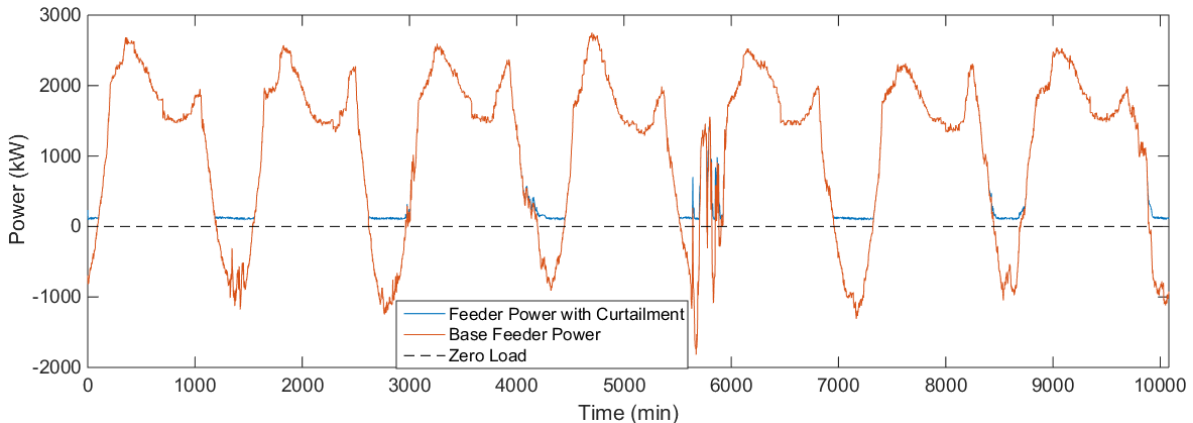


Figure 14. Substation power with and without zero-current injection control.

Although the control is commanding the PV systems to match the load during the hours it curtails, there is a small amount of real power still flowing through the feeder breaker. The output of a single PV system under ZCI control is shown in Figure 15 to investigate its performance. The inverter matches the load consumption almost perfectly, but there exists a small error. This is an artifact of the QSTS simulation, which uses the irradiance and load time series data to predict what each time step's curtailment should be rather than using measurements. This approach was taken in an effort to speed up the simulation time and results in a relatively consistent error of about 4% between PV and load power during curtailment, as shown in Figure 16. The cause of this error is most likely due to simulated load model including a slight voltage dependence where the load consumes more power at higher voltages. The load and PV power do not exactly match because the inverters are controlled to curtail exactly to the universal load multiplier time series, not the measured power of the load from the simulation results. The remaining power consumption by the feeder is shown in Figure 14. During times of curtailment is also about 4% of the overall load at those times, confirming the approximation as the source of the error. This slight under-curtailment should have a minimal impact on the overall results, however.

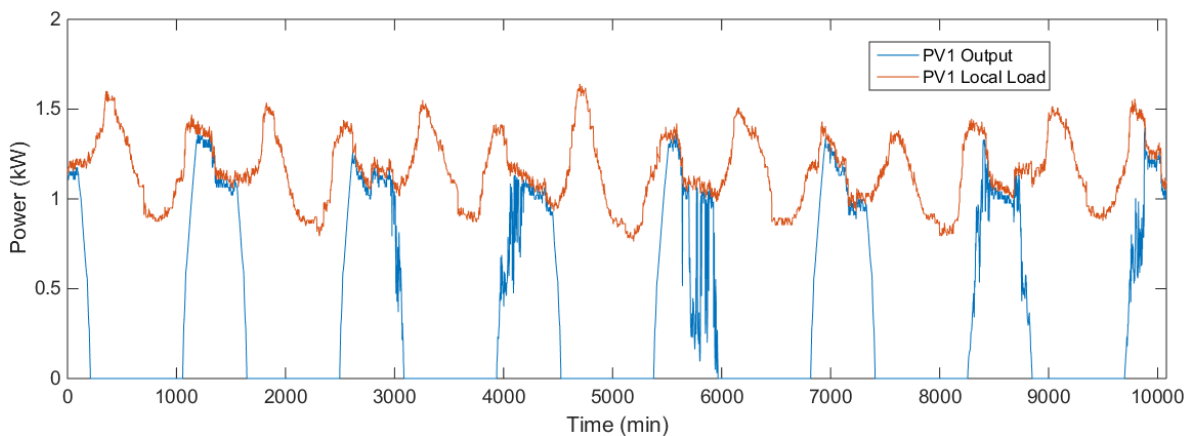


Figure 15. Power output and local load of a single PV system under ZCI control.

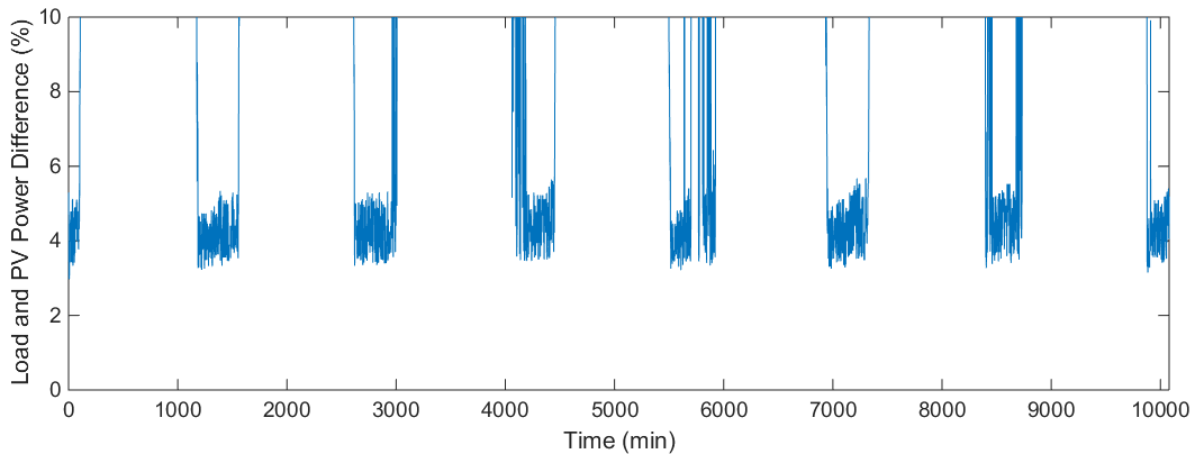


Figure 16. Percent difference in PV power output from local load consumption for a single PV system under ZCI control.

The difference in real power output of all PV systems in the network between this control and the baseline case is shown in Figure 17. With this control, the peak generating hours of each day have been shaved off to match the load.

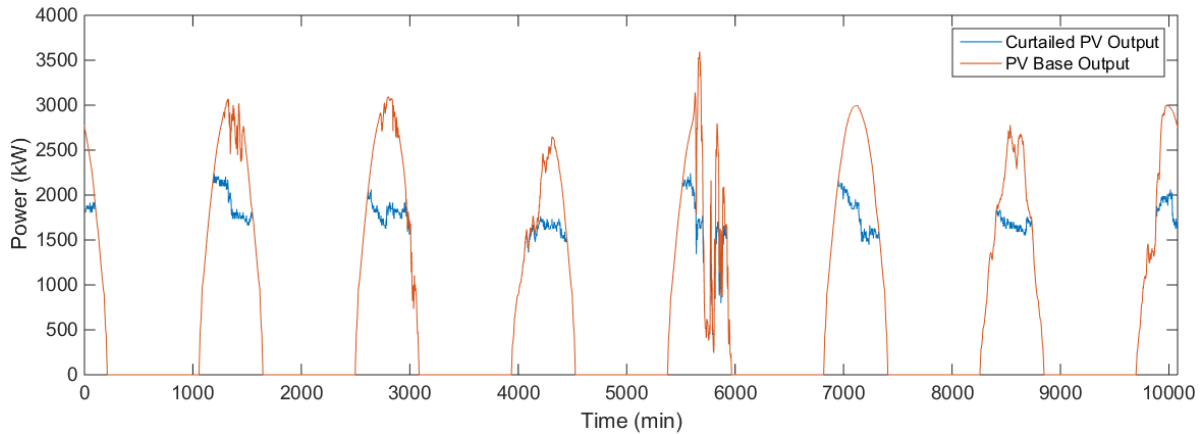


Figure 17. Total PV generation over time with and without zero-current injection control.

Using this control strategy, all over-voltage violations were mitigated for the week, but at the cost of reducing a significant amount of PV generation. With this control, a total of 6.09GWh of energy is generated over the course of the week, a reduction of 21.6% in PV production. These levels of over-voltage improvement and curtailment cost will be used as benchmarks to improve upon for more sophisticated control strategies presented in the following subsections. Although the ZCI control strategy curtails a lot of PV, it does so in a relatively fair manner amongst PV system owners. The distribution of how much each PV system curtailed from its baseline energy output during the week under ZCI control is shown in Figure 18 as the blue line. Each point in this line corresponds to the percent of the total energy a PV system curtailed due to the control. If the line is flat, it means all PV system owners have been equally curtailed relative to the size of their PV system. The “flatness” of the distribution can be measured by the standard deviation of the data. This is a relatively flat distribution with a standard deviation of only 0.75%.

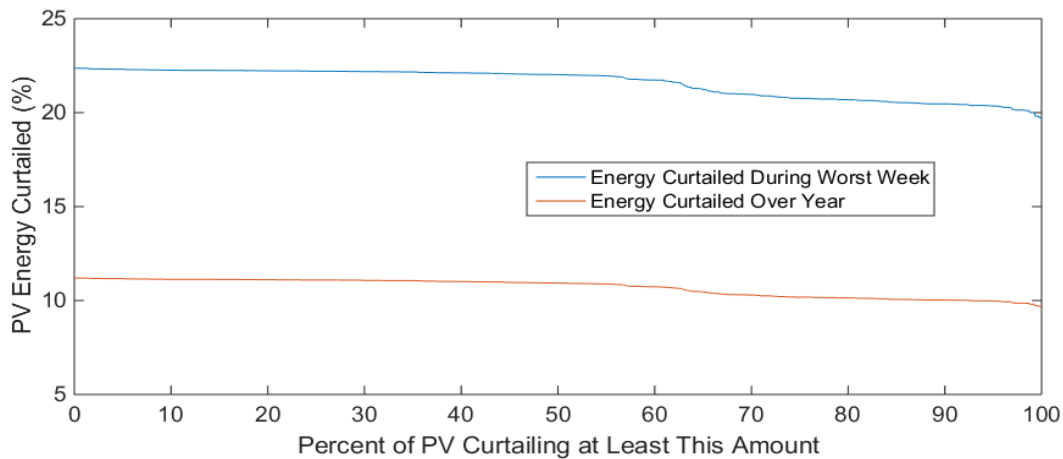


Figure 18. Disparity of PV power curtailment using ZCI control during the worst week and year.

The distribution of PV system curtailment for the year is shown as the red line in Figure 18. It has a similar shape, but is lower due to higher load on average over the year than over the one week

period studied. The year has a standard deviation of curtailment of 0.46%. No over-voltage violations occurred during the year with ZCI control, an improvement of 100%. But the cost of this improvement is an overall curtailment of 10.73% of the PV systems' potential energy production.

4.2. Local Voltage-Based PV Curtailment

For this section, the Volt/Watt control described in Section 2 is applied to each inverter. The parameter set $\mathbf{v} = [v_1, v_2]$ that defines the controller Volt/Watt curve in Figure 1 is tuned using the worst week of data in the year. Ten parameter sets are tested using $v_2 = 1.05$ and linearly varying $v_1 = [1.040 \dots 1.049]$. The performance of each parameter set is summarized in Figure 19. The top plot shows the percent of the week the network spent in an over-voltage violation, which should be zero for a successful control performance. The bottom plot shows the percent by which the total PV power generation is curtailed due to each control. As expected, a lower v_1 parameter corresponds to more curtailment, yet the increase in voltage violations as v_1 increases is not readily explained since each inverter should curtail completely by the time the voltage limit is hit locally. These higher v_1 settings correspond to larger controller gains, so one possible explanation is poor interaction between the inverters and other feeder voltage regulation. Alternatively, the QSTS solution may not be converging to a single operating point if the parameters that determine maximum controller rate of change and convergence tolerance are not set properly for these higher gain values. To investigate the cause of these over-voltages further, the time-domain cumulative power outputs corresponding to parameter Sets #5-10 are plotted in Figure 20 for a midday time period with some irradiance variability. It is evident that some of the parameter settings are causing the inverters to oscillate between output levels as the irradiance varies. This is an indication that the controls are not achieving a stable operating point. It seems in this case that the larger controller gains associated with the higher v_1 parameter cause the inverter controllers to take too large of steps between solution iterations and never find the stable operating point.

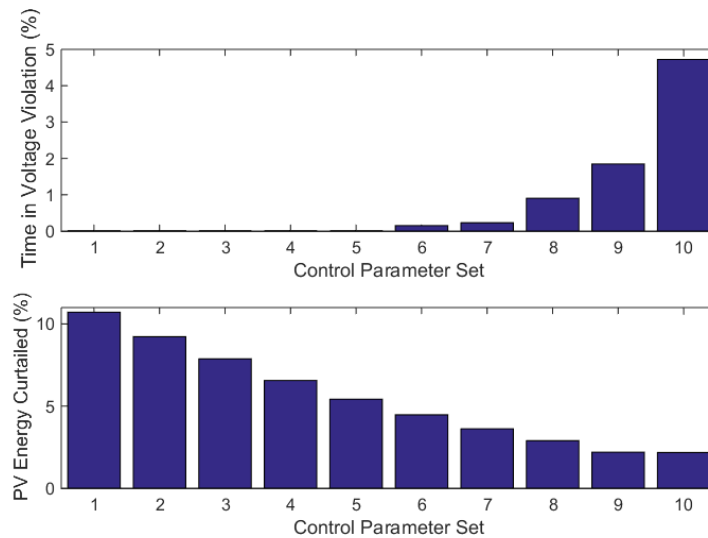


Figure 19. Comparison of the performance during the worst week for different local control parameter sets.

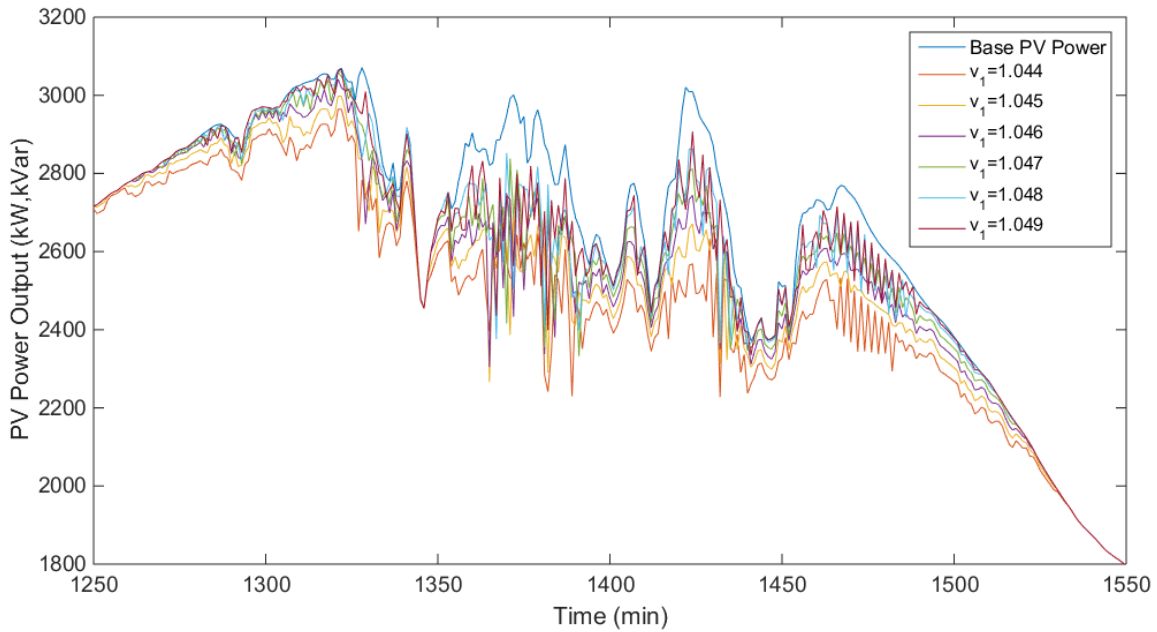


Figure 20. Impact of Volt/Watt control parameters on power oscillations due to irradiance.

For this reason, the maximum rate of change in inverter power output between control iterations is lowered in OpenDSS from 40% to 10% of the inverter rating and the tuning procedure is run again. Since the original tuning procedure already discovered that voltage violations are mitigated at $v_1 = 1.044$, only six parameters within the set $v_1 = [1.044 \dots 1.049]$ are tested this time. The comparison of the performance of this reduced set of parameters is shown in Figure 21. Now all voltage violations are mitigated up to $v_1 = 1.046$ (Set #3), which means even less power needs to be curtailed to mitigate violations with the control working properly.

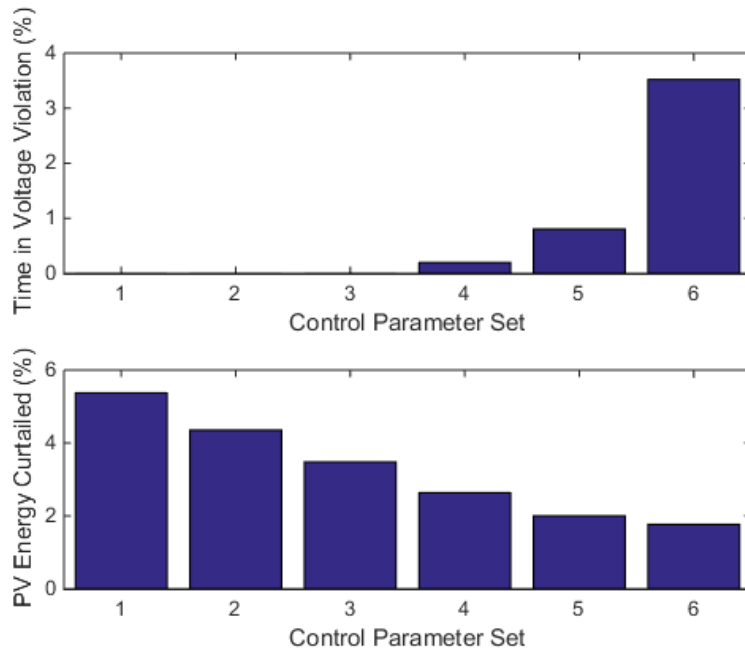


Figure 21. Volt/Watt control parameter comparison with lowered maximum power rate of change.

It remains unclear, however, why Sets #4-6 still have voltage violations in Figure 21. The same time period as in Figure 20 is investigated to see if the inverters are still struggling to find stable operating points at higher gains. As shown in Figure 22, it appears that the inverters are no longer oscillating between operating points during periods of highly variable irradiance. In this case, it seems there is another cause for the voltage violations at the highest controller gains. It could be that there are still some inverters that oscillate between stable settings, but the magnitude of the oscillations has been decreased from 40% to 10% and averages out among all PV and is no longer visible. Alternatively, the inverters could be allowed to run at full output so closer to the ANSI limit at the highest settings that only one instance of over-voltage could bring the 10-minute average into violation.

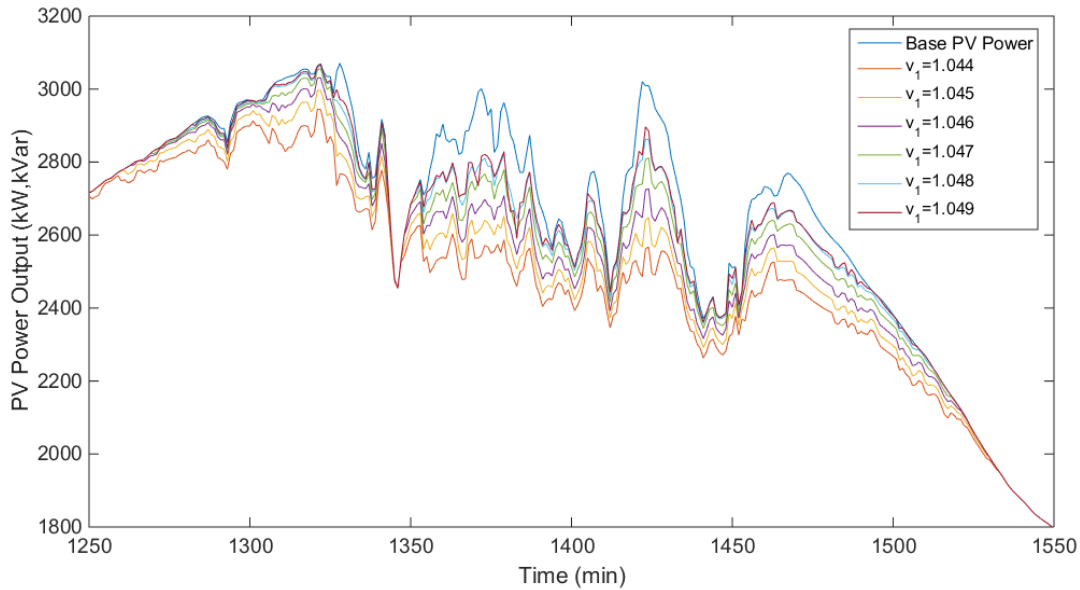


Figure 22. Impact of Volt/Watt control parameters on PV system power output with lowered inverter maximum power rate of change.

Since it remains unclear why higher v_1 settings still produce voltage violations, the control parameters are conservatively set at $v = [1.045, 1.05]$ to reduce the chance of incurring over-voltages in the full year simulation. The control's curtailment of the baseline PV system power output during the worst week is shown in Figure 23. Over the week, Volt/Watt control with these parameters mitigated 100% of over-voltage violations and curtailed 4.35% of the energy that would have otherwise been generated with no control. This is a much reduced value from the previous local control of zero current injection. However, these improved results are not as fair to all customers as the ZCI approach. The blue line in Figure 24 represents the distribution of PV curtailment due to Volt/Watt control during the worst week and it can be seen that a small portion of the PV systems curtail much more than the majority. If the goal is to limit PV system curtailment to 10%, then 17.5% of the customers on this network will curtail more than this value, with the maximum curtailment up to 36.8% of its potential energy production. The PV systems interconnected to the most robust lines do not have to curtail any power under this control, which is why the average curtailment is so low at 4.27%. Although the performance of this control is superior, it introduces the discussion of whether it is better to collectively curtail more power for the sake of fairness.

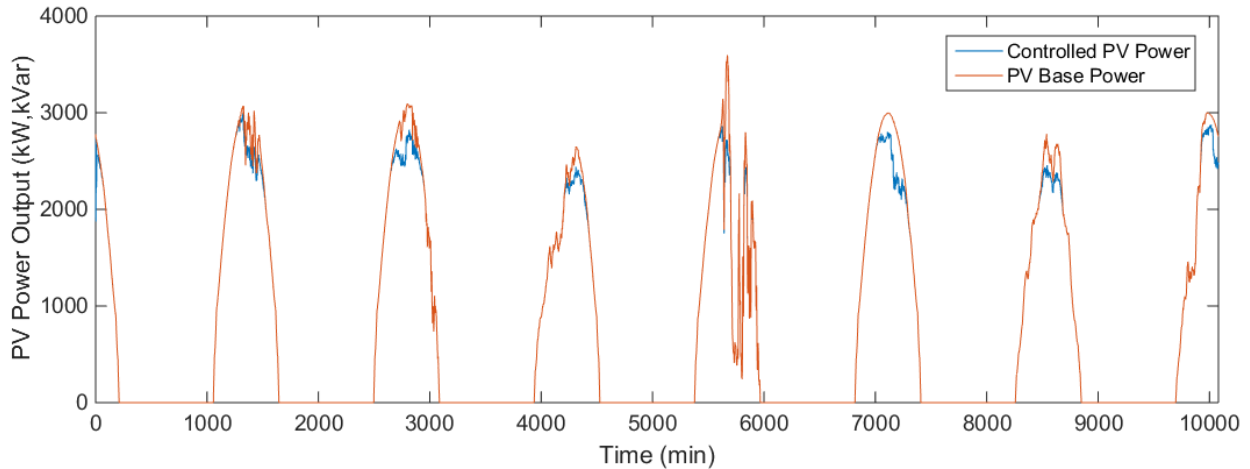


Figure 23. Total PV power generation during worst week with tuned Volt/Watt control.

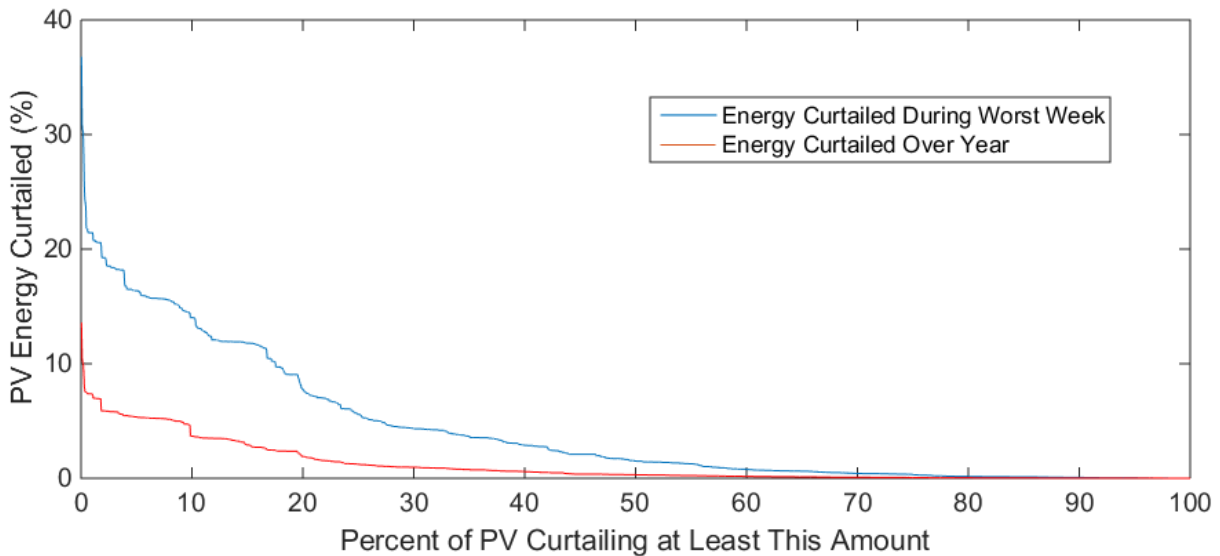


Figure 24. Disparity of PV power curtailment using Volt/Watt control during one week and over one year.

Running the entire year with the above tuned controller parameters is also successful in achieving zero over-voltage violations. Also, the relative amount of control action needed is greatly reduced when averaged over the year. To achieve this improvement, the PV systems only needed to be curtailed by 0.85% of their cumulative baseline energy output over the year. This represents the amount of energy curtailed by the control that would have otherwise been produced by the PV systems during the entire year. The amount of energy curtailed during each day of the year can be seen in Figure 25. However, as with the one-week case, the disparity in the curtailment of the PV systems is large, as shown in the red line of Figure 24. The maximum amount of curtailment seen by a single PV system is 13.57% and the minimum is less than 0.001%. However, the previously stated goal of curtailing less than 10% of available energy is achieved by 99.7% of the PV systems. The standard deviation of the distribution of PV curtailment is 1.81% for the year using this control.

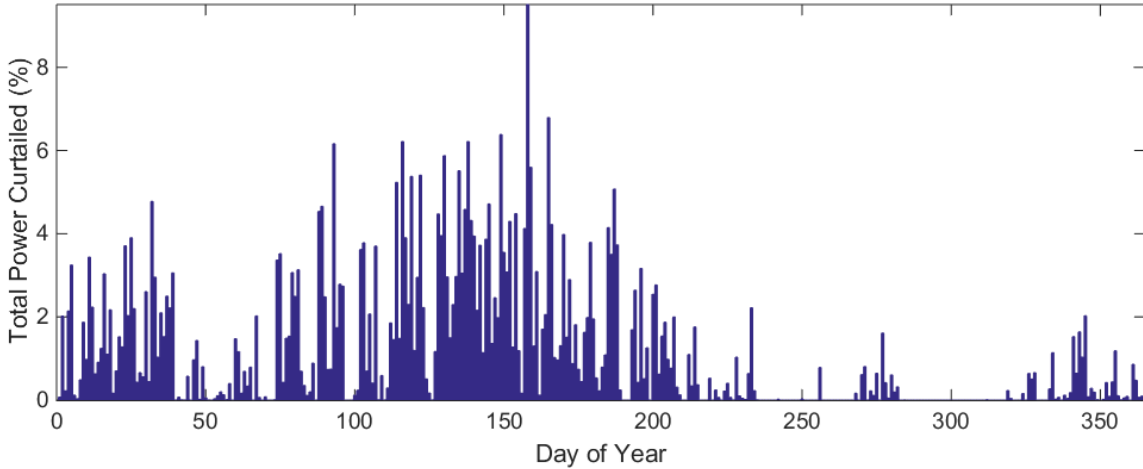


Figure 25. Total curtailment of PV energy during each day in the year under Volt/Watt control.

Looking at the curtailment of each PV system based on its location in the feeder in Figure 26 highlights the clustering of PV systems facing the highest control costs. The worst-week data has been used since it has a larger disparity that will be more visible, but the full year results are similar. Each point represents how much energy the PV system at that location had to proportionally curtail over the week due to the Volt/Watt control. The highest curtailments occur in a cluster of loads on a lateral branching off near the substation. The next highest curtailments occur towards the end of the feeder, as is to be expected due to the voltage rise effect along the entire feeder.

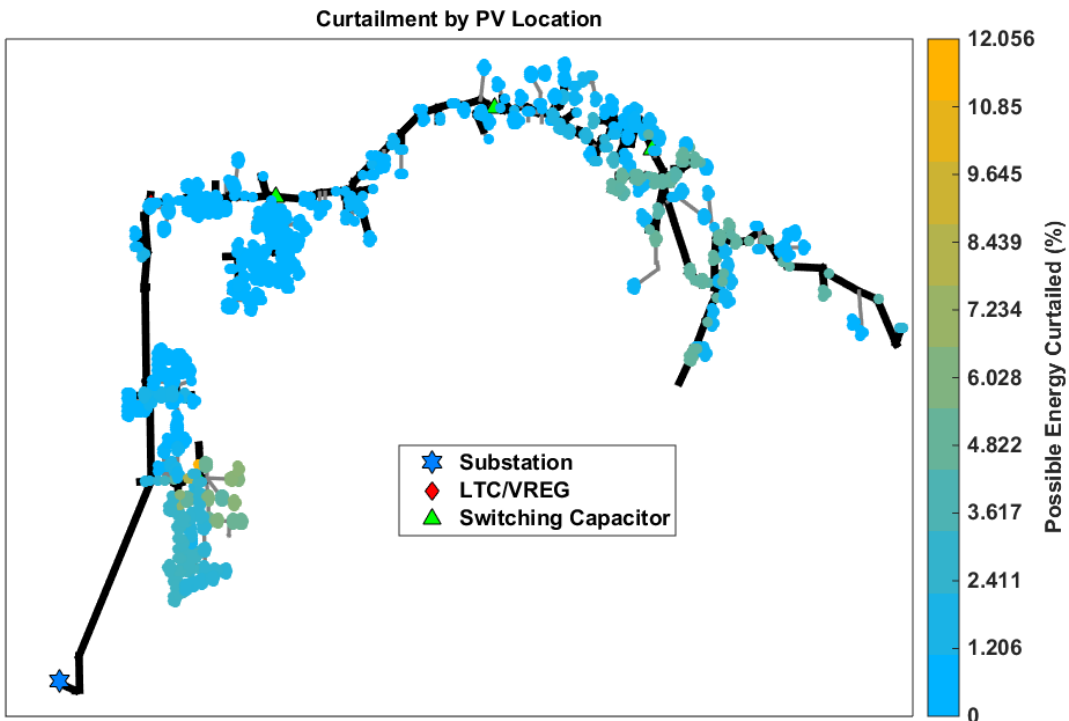


Figure 26. Geographic distribution of PV system curtailment in the circuit due to Volt/Watt control.

The curtailment levels don't correspond to the presence of large PV systems, but rather due to existing poor voltage profiles. This is evident in Figure 27 where it can be seen that relatively few large PV systems are present in the feeder branch that experiences the worst curtailment. However, the voltage profile of this branch is the worst in the network as it is before the voltage regulator and possibly due to poor control of the local capacitor bank. A zoomed-in plot of this branch in Figure 28 shows the PV systems nearest to and downstream of the capacitor curtail the most.

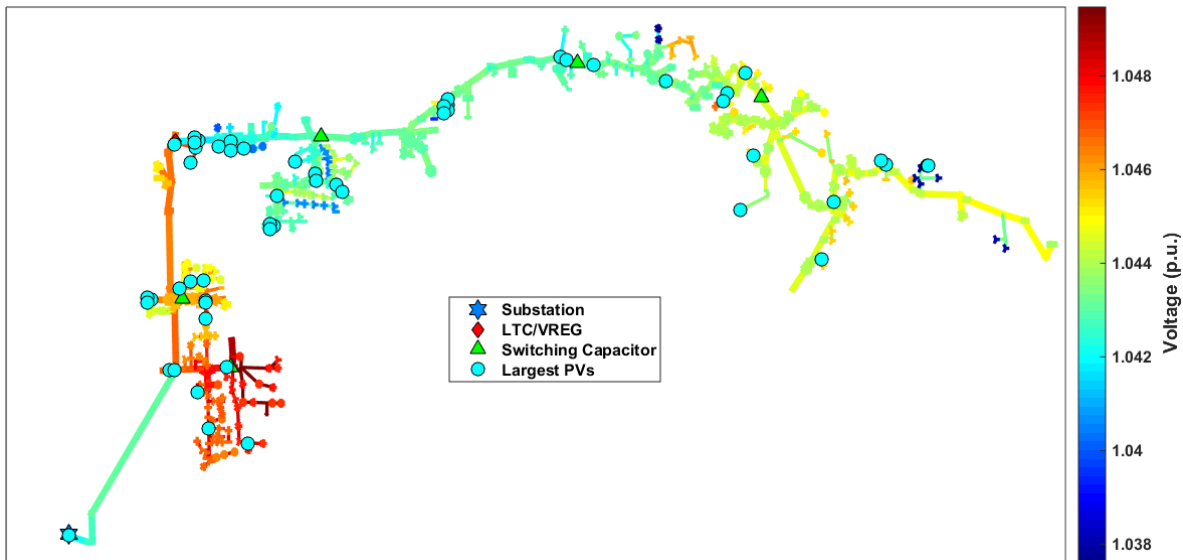


Figure 27. Distribution of largest PV systems in the circuit and relative line voltages.

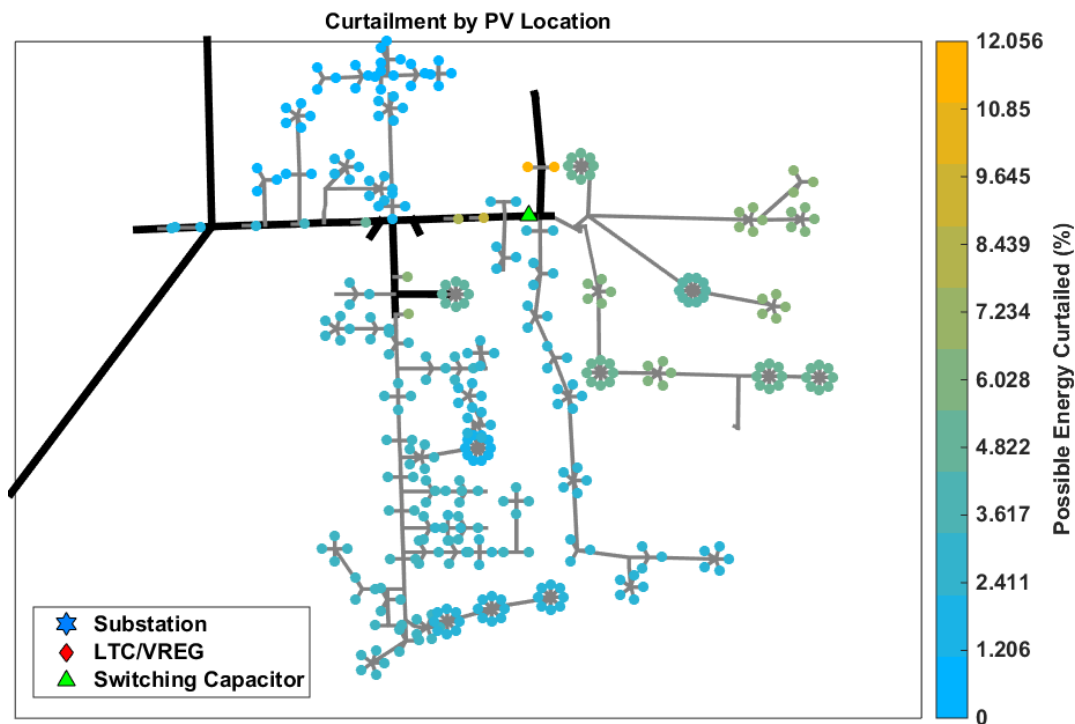


Figure 28. Zoomed section of highest curtailment in feeder due to Volt/Watt control.

4.3. Local Voltage-Based Var Control

This section demonstrates the effectiveness of implementing local reactive power support on the PV inverter by itself. The control strategy implemented is the Volt/Var control described in Section 2.2. The inverter is assumed to be rated the same size as the PV panels, however, OpenDSS has a convergence problem when setting these parameters equal and implementing Volt/Var control. Therefore, the ratings of the PV inverters in the simulation are increased by 1%. This change should not significantly impact the results.

The time-domain total power output of the PV systems is shown in the top plot of Figure 29. The inductive vars are plotted against the real power generated for clarity since it is assumed the vars will always be inductive due to voltage rise. The Volt/Var controller does not affect the real power output of the PV system but absorbs reactive power through the inverter when it turns on. The control does not operate at night because the inverters shut off below 10% real power output. This practice is common as most inverters do not operate efficiently at low power. The subsequent over-voltage violations that occur on the network are shown in the bottom plot of Figure 29. The only period of voltage violations occurs midway through the week. When compared to the top plot, this coincides with a point where the real power output of the PV spikes and is preventing the control from supplying enough reactive power. It may seem as though the inverters are outputting a lot of reactive power, but it should be noted that the PV systems consistently operate below their peak ratings. In fact, looking at all the irradiance multipliers in Figure 30 for the week, it is clear that only a few brief minutes in the week do some PV systems see enough irradiance to provide rated power output. In fact, the period in which the voltage violations occur does not even coincide with one of these times, but still limits the reactive power enough due to the manner in which the profiles are distributed among the PV systems at that point.

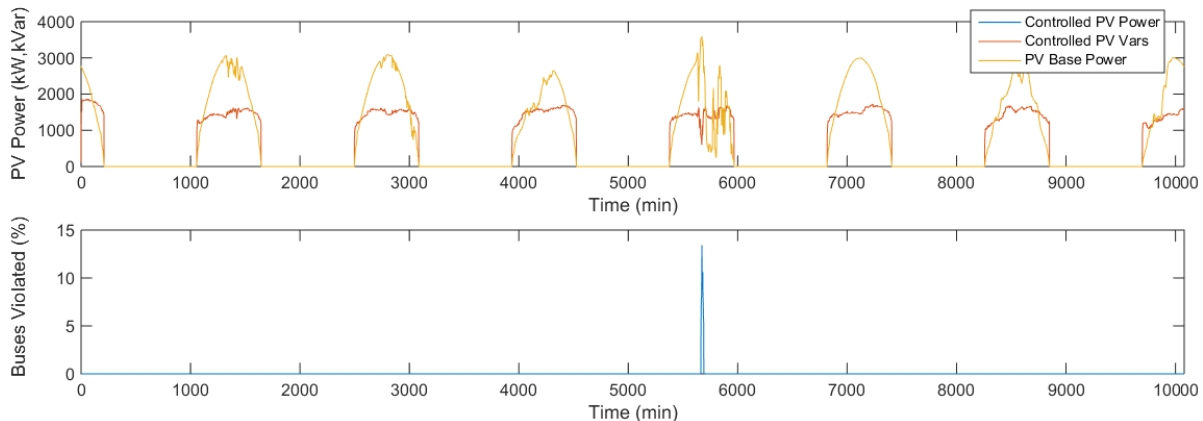


Figure 29. (top) PV real and reactive power output during worst week of voltage violations with Volt/Var control. (bottom) Total voltage violations seen on feeder with Volt/Var control.

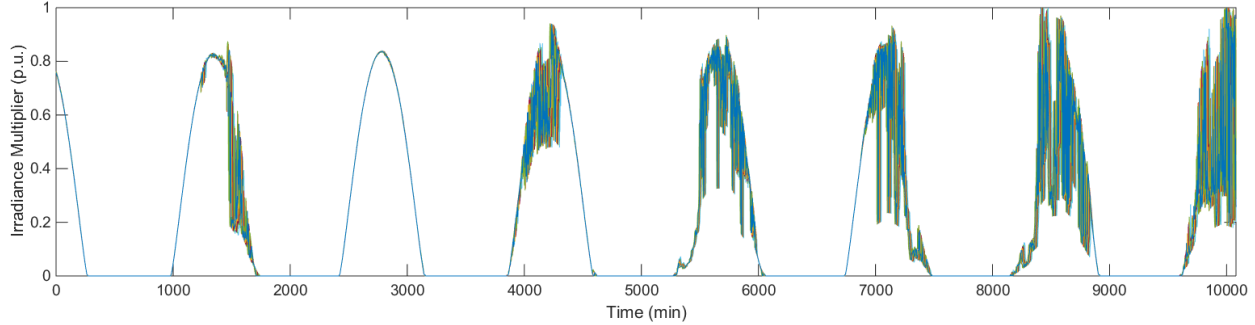


Figure 30. All irradiance multiplier time series for worst week of voltage violations.

Even with the time period where the control fails to prevent over-voltages, these results are very encouraging. With only Volt/Var control, the feeder is only in over-voltage violation for 28 minutes of the week, or 0.28% of the time, corresponding to an overall reduction in 97.9% of violations. The indication here is that with reactive power support, the PVs should only need to curtail during this 0.12% of the year to mitigate all voltage violations. The results for running the entire year of data are similar with the feeder in violation only 624 minutes of the year, or 0.12% of the time. This represents a 96.7% reduction of the voltage violations seen in the no control case.

4.5. Centralized Fair Curtailment Dispatch

One-minute Dispatch

This simulation applies the control strategy discussed in Section 2.3. It leverages a centralized communication structure to gain knowledge of the maximum voltage in the network but dispatches the curtailment signal equally to all inverters as a proportion of their maximum rating. Since there are two distinct control parameters, the sets of control parameters tested do not follow a continuous range as in the local control case. An initial attempt at tuning the centralized regulator gains is made as follows. Parameter Sets 1-5 and 16-20 use an inertia gain of $K_{\Phi} = 1.0$ while sets 6-10 use $K_{\Phi} = 0.9$ and sets 11-15 use $K_{\Phi} = 1.1$ to test this gains impact. Sets 1-15 use a regulator gain of $K_R = [1 \ 5 \ 10 \ 20 \ 30]$ while sets 16-20 use regulators gains of $K_R = [50 \ 60 \ 70 \ 80 \ 90]$ to see if higher values are viable. The results of the different parameter sets are shown in Figure 31. The first thing that should be noted from the top plot is that none of the parameter sets were able to completely mitigate all over-voltage violations using this control. It appears that parameter set #15 mitigates most violations at a minimal curtailment cost, however, the fact that slightly lower regulator gains using this same inertial gain curtailed nearly all PV system output is worrisome. Since using this type of control in the QSTS simulation is similar to a discrete control system, using a regulator gain of $K_{\Phi} > 1.0$ may be unstable. The other parameter combinations all have voltage violations above what would be considered a successful control strategy. For this reason, another attempt at parameter tuning is made. Additionally, the higher set of regulator gains $K_R \geq 50$ can be discarded due to the level of oscillation in the control they cause, as shown in Figure 34.

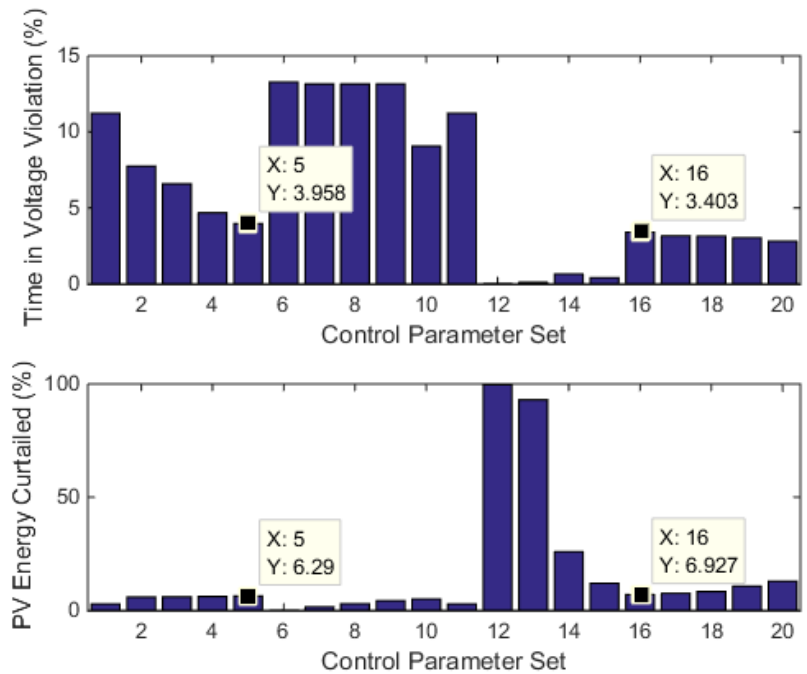


Figure 31. Comparison of the performance of an initial set of different central fair control parameter sets.

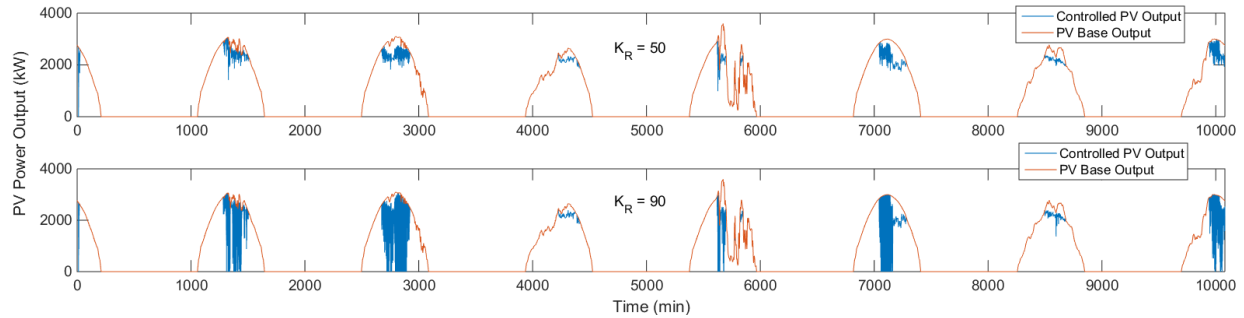


Figure 32. Result of increasing regulator gain from lower value (top) to higher value (bottom).

These results bring to light the importance of the voltage limit being regulated to, or V_{lim} in (1). Since each voltage violation is a 10-minute average, regulating the PV power outputs to be exactly at the limit means they would spend time above the limit, making averages above the limit a likelihood. For the next tuning attempt, parameter Sets #1-5 use $V_{lim} = 1.049$ and Sets #6-10 use $V_{lim} = 1.048$ and both subsets use the regulator gains of $K_R = [1 \ 5 \ 10 \ 20 \ 30]$ and inertia gain $K_\Phi = 1.0$, which were determined to be the more stable of the previous approach. The comparison of the performance of these sets is shown in Figure 33.

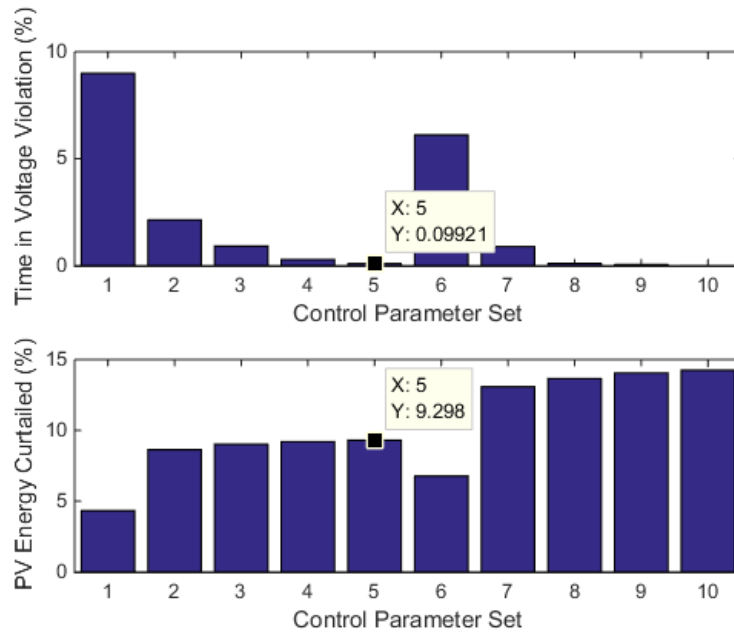


Figure 33. Comparison of the performance of the updated central fair control parameter sets.

There is a distinguishable trade-off between the two voltage limits. The parameter sets on the left, corresponding to $V_{lim} = 1.049$ curtail less power, but do a poorer job of mitigating voltage violations, as expected. In both cases, as the regulator gain increases, the number of violations decreases. Both parameter sets #5 and #8-10 are viable, since they are near zero for voltage violations, and since Set #5 represents the minimum curtailment, it should be selected. First, the time-domain performance of these parameter sets is investigated. The top plot of Figure 34 shows how the parameter sets corresponding to $V_{lim} = 1.049$ behave during a time of highly variable irradiance and the bottom plot shows the behavior of the sets corresponding to $V_{lim} = 1.048$. The increase in curtailment caused by lower regulator voltage limit is evident in the bottom plot. The regulation action in the top plot, however, seems to have times where it oscillates with more aggressive regulator gains. The oscillations increase with higher gains, but even at the highest gain tested, the magnitude of the oscillations is less than 10% of the cumulative output. This overall impact can be seen in the performance of the control at the parameters over the entire week in Figure 35. It should also be noted that these are not dynamic oscillations but rather an oscillating dispatch signal. Therefore, this set of parameters is used for the full year simulation since it results in objectively better performance overall. Over the week, the feeder is in violation 0.10% of the time, which is a 99.2% improvement from the base case. Across the feeder, the number of violations at buses with PV systems is reduced to 69, an improvement of essentially 100%. The control curtails 9.30% of the energy available to the PV systems to achieve this, but it does it in a fair manner with a disparity in curtailment that has a standard deviation of only 0.57%. The distribution of curtailments during the worst week is represented by the blue line in Figure 36.

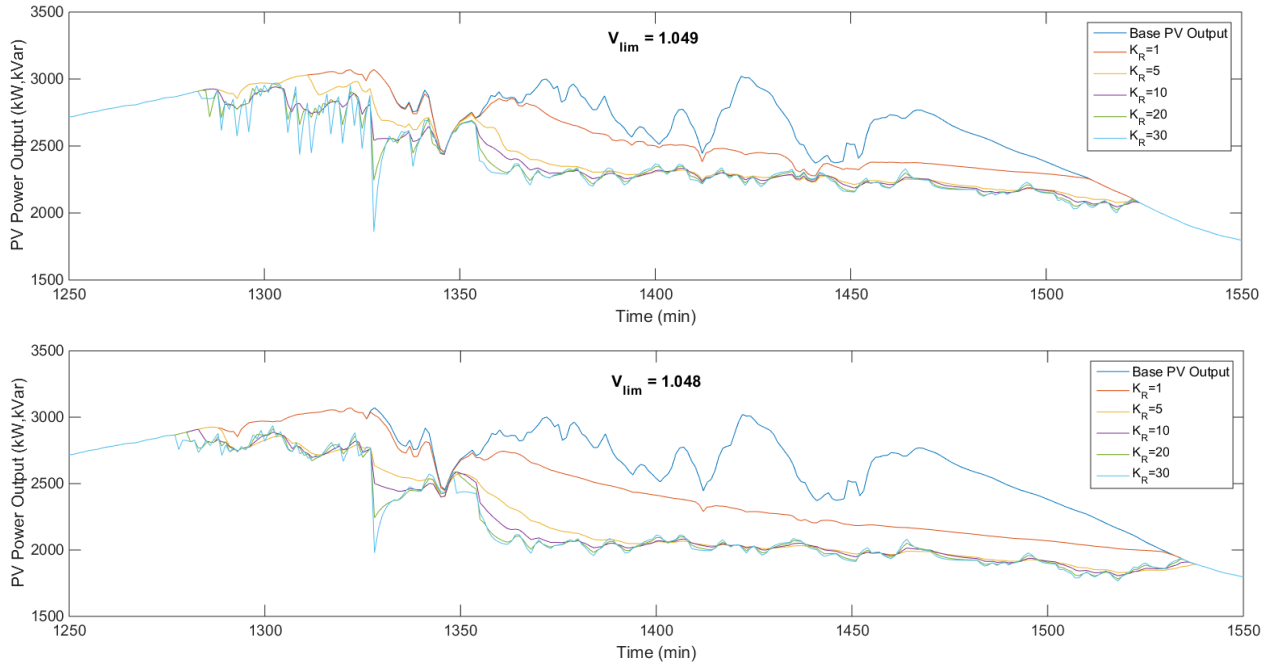


Figure 34. Centralized fair curtailment control time-domain performance comparison for (top) $V_{lim}=1.049$ and (bottom) $V_{lim}=1.048$.

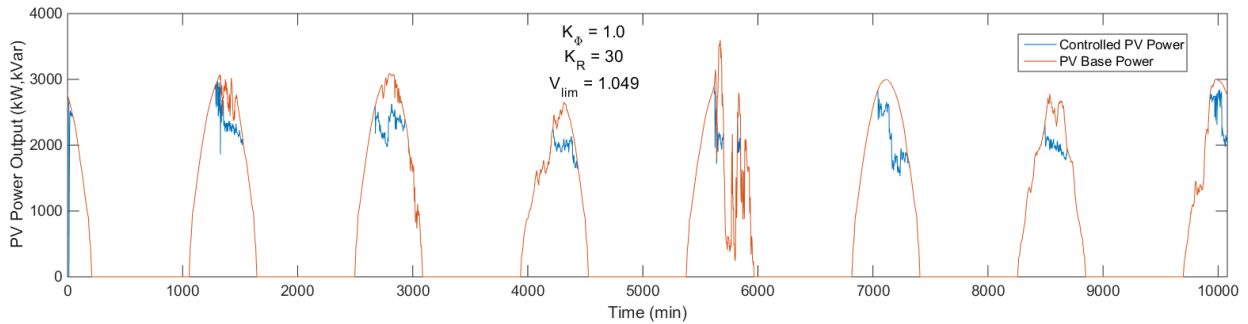


Figure 35. PV power output using tuned fair dispatch control parameters during the worst week.

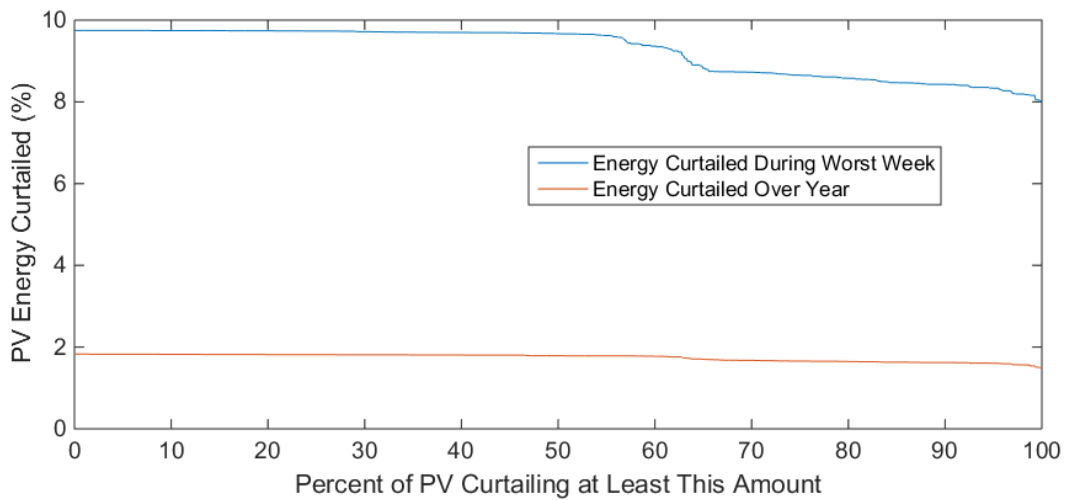


Figure 36. Disparity in PV power curtailment using fair centralized dispatch during worst week.

Using the selected controller parameters, the QSTS simulation is run for the full year of data with the centralized fair curtailment control. As expected from the control’s performance during the worst week, the control is unable to mitigate all over-voltage violations, but it is able to mitigate most of them. The amount of time per day spent in over-voltage violation throughout the year is shown in Figure 37. Only 33 days of the year see a voltage violation and the feeder is in violation for only a few minutes during those days. Looking at how prevalent these violations are throughout the feeder in Figure 38, it can be seen that no more than 2% of the buses are ever in violation. The PV power curtailed during each day of the year is shown in Figure 39 and the disparity in curtailment between PV systems is shown in Figure 36 as the red line. Again, this control type distributes the responsibility of reducing voltage violations fairly among all PV systems. The standard deviation in curtailment between PV systems is only 0.09%. This flat distribution of curtailment can be further visualized by plotting the relative amount each PV system curtails within the circuit map as in Figure 40. Although the variation is very slight, it is interesting to note the east-west transition in curtailment, which mirrors the irradiance delay imposed in Figure 7. Overall the feeder is in violation 0.02% of the year, corresponding to a 99.3% reduction in time spent in violation. The total number of violations has been reduced to 391 minutes over the year, which is nearly a 100% improvement. The PV systems curtailed 1.75% of their total energy production to achieve this result. Given this relatively low curtailment over the year, the control could potentially use the lower $V_{lim} = 1.048$ setting to potentially mitigate all voltage violations over the course of the year.

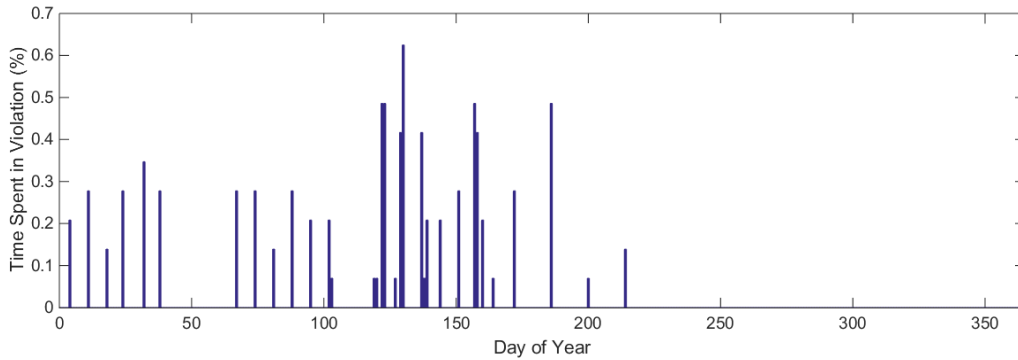


Figure 37. Percent of time feeder is in violation during each day of the year under fair curtailment.

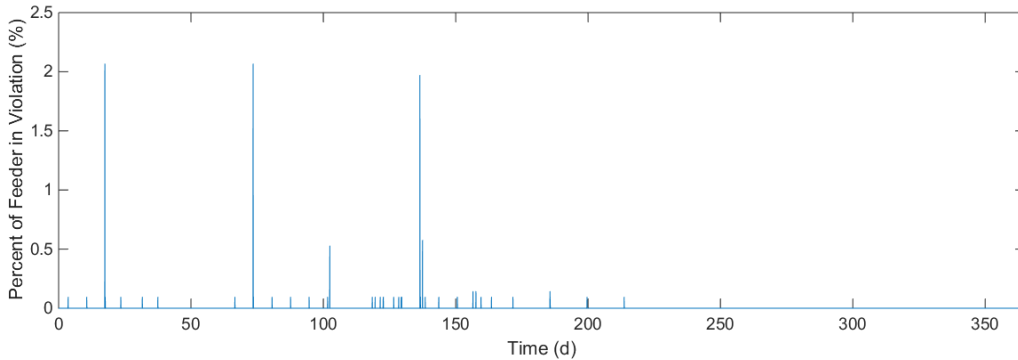


Figure 38. Percent of feeder in voltage violation during the year under fair curtailment.

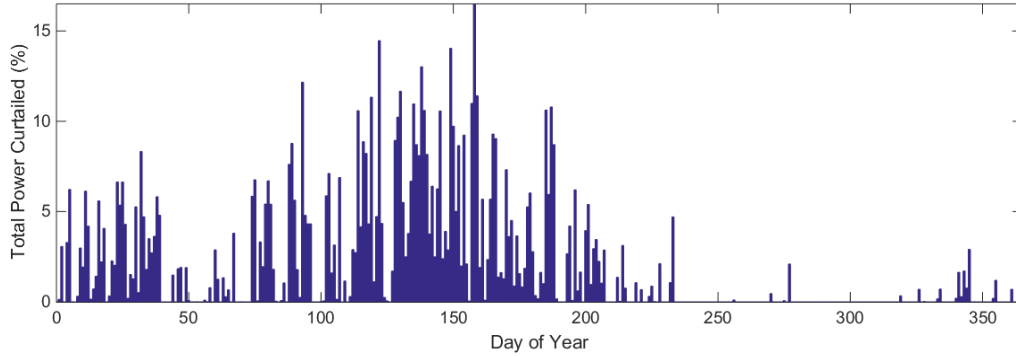


Figure 39. Percent of total PV system power output curtailed during each day of the year under fair curtailment.

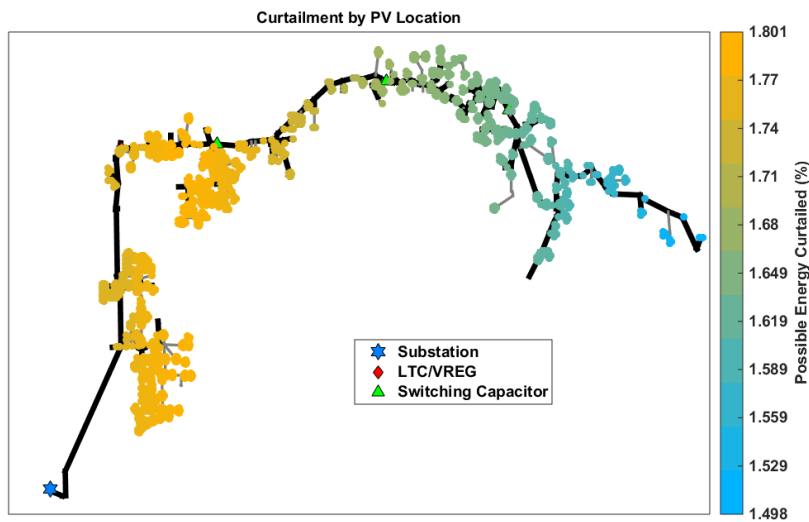


Figure 40. Geographic distribution of PV system curtailments in the circuit due to fair dispatch control.

Five-minute Dispatch

It is of interest to increase the time in which the centralized controller is assumed to be capable of dispatching a signal to all inverters to see how this may impact the performance of the control. Due to the previous results, the inertia gain is kept at a constant $K_{\phi} = 1.0$ with $V_{lim} = 1.049$ and only the regulator gain is adjusted within the set $K = [1 \ 5 \ 10 \ 20 \ 30 \ 50 \ 60 \ 70 \ 80 \ 90]$. The resulting over-voltage violations and PV system power curtailments at these various gains are compared in Figure 41. Based on the consideration that the power curtailment should not exceed 10% of the PV system's base value, parameter sets #4-10 are disqualified. Sets #1-3 are then compared by observing their curtailment behavior during the entire week in Figure 42 and for a single day in Figure 43. Nothing abnormal stands out from the weeklong simulation, but looking at a single day it is clear that Set #3 shows much more oscillation than the other two. With the next control goal being to minimize voltage violations, Set #2 is chosen to set the regulator gain to $K = 5$ for the five-minute dispatch. As expected, this is lower than the gain selected for the regulator using a one-minute dispatch window.

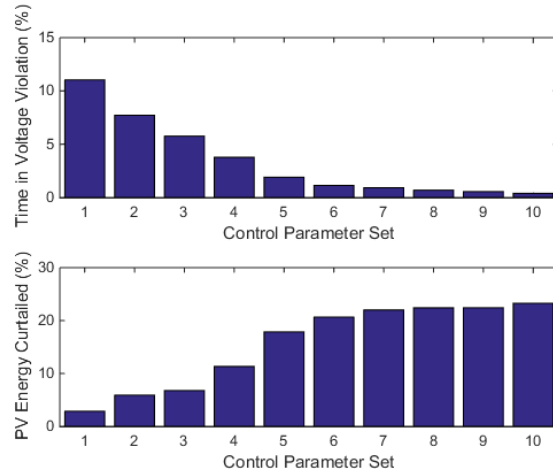


Figure 41. Comparison of the performance of different fairly dispatched control parameter sets under five-minute dispatch.

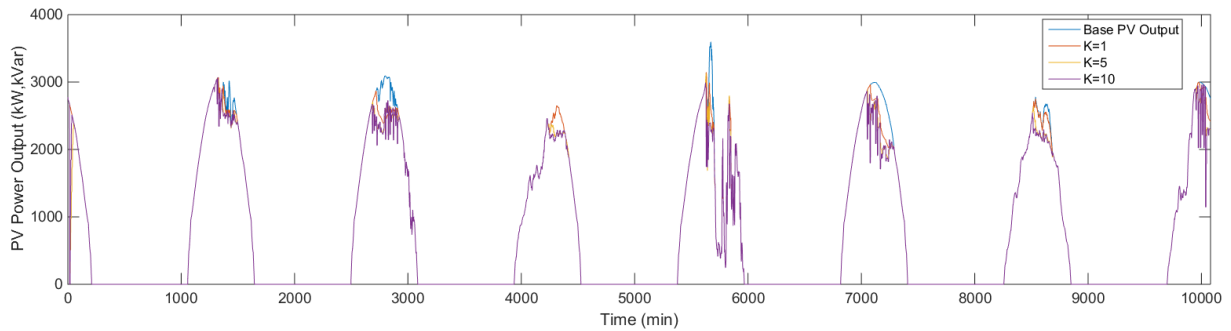


Figure 42. Curtailment comparison of three different control parameters for fair dispatch control under 5-minute dispatch window.

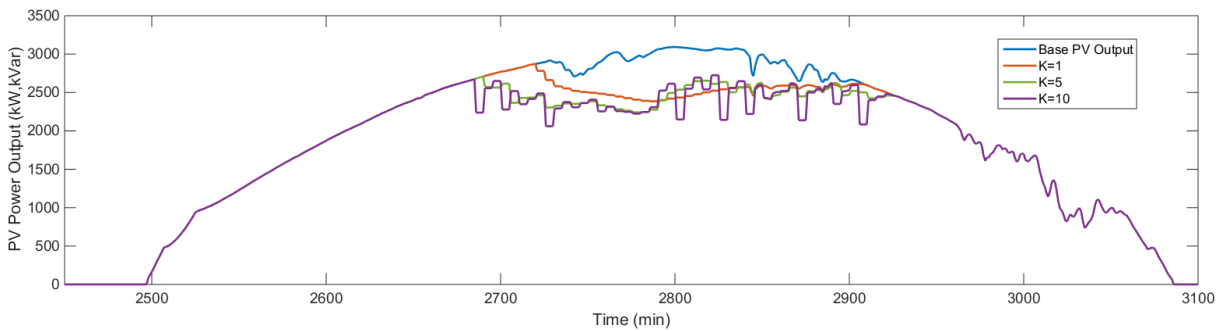


Figure 43. Comparison of a single day of fair dispatch control operating with 5-minute dispatches under three different regulator gains.

This control has over-voltage violations 7.65% of the time, representing a 92.3% mitigation in total voltage violation occurrences and a 41.9% improvement in time spent by the feeder with any violation. The cost of this control is a 5.89% curtailment in total PV system power generation. However, as expected, this control action is evenly distributed among the PV systems, as shown in Figure 44. The standard deviation in the distribution of curtailment is 0.16%. Over the year, a gain of $K = 10$ is used after it is found that $K = 5$ is not aggressive enough during the rest of the year and yields poor results without much curtailment. With the increased gain over the year, the control reduces all violations by 97.6% and the time the feeder

spends in violation by 88.4% while curtailing 2.00% of the total PV system energy production. The standard deviation in the distribution of curtailment is 0.05% over the year.

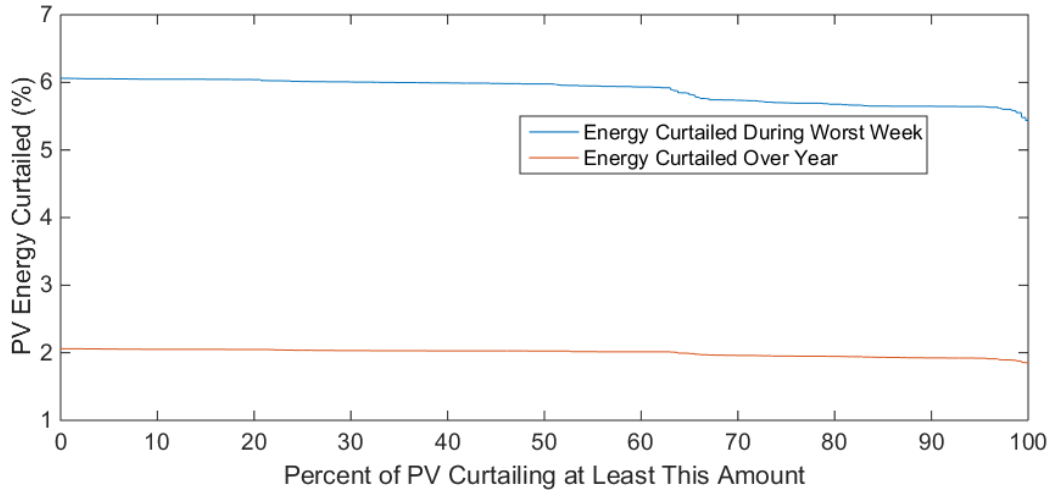


Figure 44. Disparity in the amount of power curtailment seen by the PVs under fair centralized control with a five-minute dispatch window.

4.7. Curtailment Dispatch via PV Voltage Sensitivities

One-minute Dispatch

This control strategy also assumes real-time measurements from all PV systems are available to the centralized control at one-minute time steps and the controller can dispatch desired power output levels to each individual PV system at some variable time step. The details of this curtailment strategy are presented in Section 2.4. The main difference between this control and the one proposed in Section 2.3 is that fairness in curtailment or control action used between PV systems is not considered a priority. Rather, the main goal of this control is simply to mitigate the PV-induced voltage violations with as little cumulative curtailment as possible. This is achieved by assuming some knowledge about the distribution network, namely, the sensitivities of the PV systems' power outputs to the network voltages.

A sensible choice for the voltage to regulate to is $V^* = 1.05$, so it remains constant to simplify the controller tuning. Twenty parameter sets are selected to tune the controller. Sets #1-5 and #11-15 use $K_A = 1.0$ and the rest use $K_A = 1.1$ to test how a slightly more aggressive use of the sensitivities will affect the results. Each subset of five parameter sets use the range of change of power limiter $\Delta P_{lim} = [0.1, 0.2, \dots, 0.5]$. A comparison of the different control parameter sets used to tune the regulation of the curtailment parameters is presented below in Figure 45. The first thing to note from the top plot is that even though parameter set #13 did completely mitigate all voltage violations, the magnitude of all the other voltage violations is miniscule. In fact, these violations may even be considered negligible when it is considered that the local control that mitigated all voltage violations in tuning still had a few during the entire year simulation. With that said, parameter set #13 achieves this slight improvement at the cost of nearly 50% more curtailment than some of the other sets. For these reasons, parameter set #10 is chosen for the

controller tuning, which corresponds to a sensitivity gain of $K_A = 1.1$ and a curtailment change limit of $\Delta P_{lim} = 0.5$. For the worst week, this parameter set had voltage violations 0.05% of the time. This represents an overall violation improvement of essentially 100.0% and a 99.6% improvement in time spent in violation at the cost of curtailing the cumulative PV output by 3.99%. The performance of this controller over the course of the week is shown in Figure 46. There is a low amount of curtailment without any visible regulator oscillation. However, the downside of the manner in which this control achieves these improved results is apparent in the plot of PV system power curtailment disparity, represented by the blue line in Figure 47 for the week. Under this control, there is a standard deviation of 8.21% and one PV system owner has the amount of energy they generate curtailed by over 80%. This is by far the least fair of the control types.

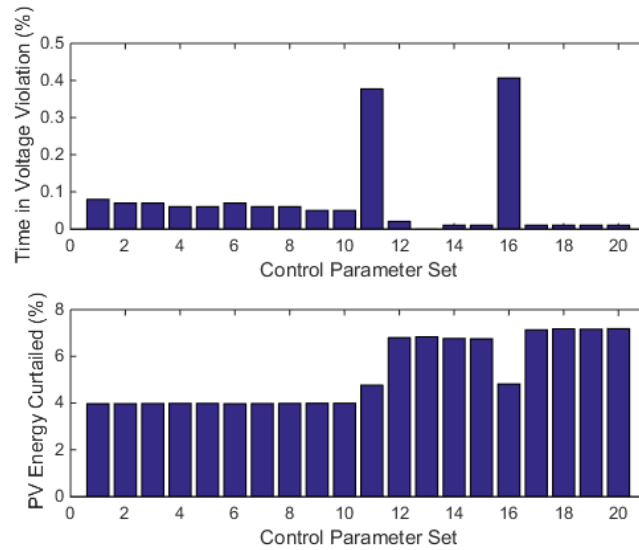


Figure 45. Comparison of the performance of different sensitivity-based control parameter sets.

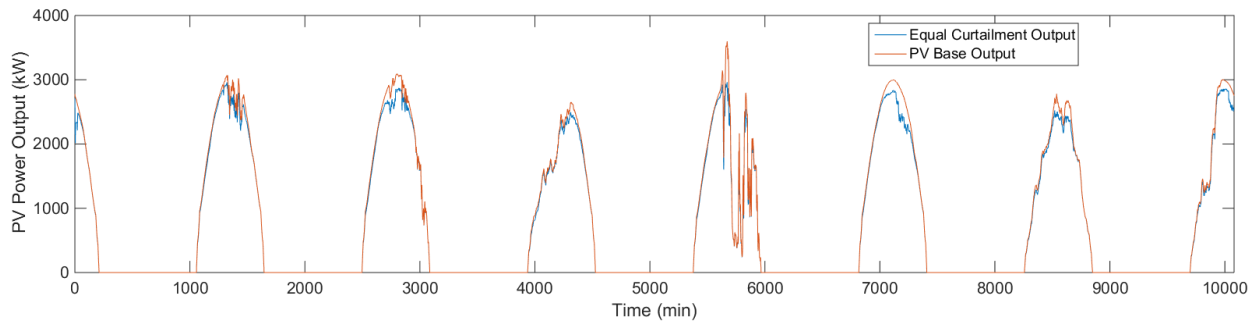


Figure 46. Worst week time series PV curtailment using centralized sensitivity-based PV dispatch at 1-minute intervals.

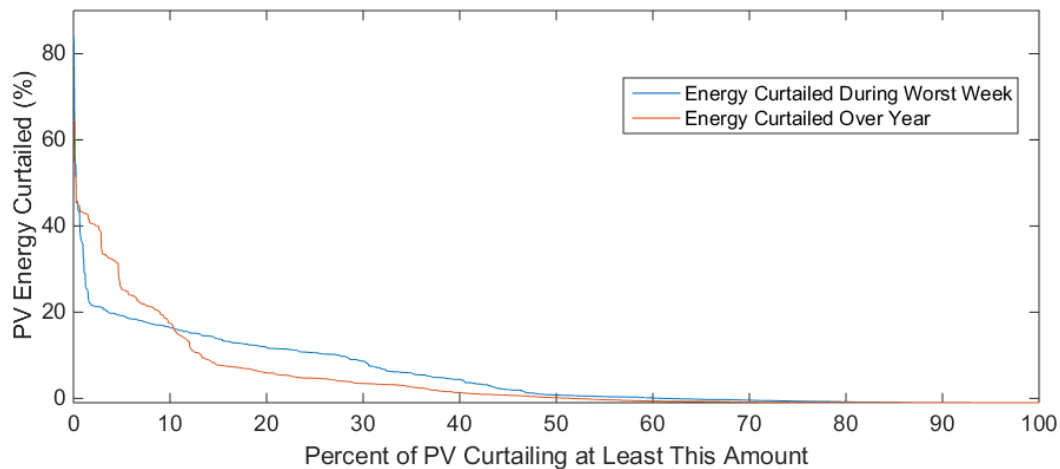


Figure 47. Disparity in the amount of power curtailment seen by the PVs under sensitivity-based control.

Over the year, the one-minute sensitivity-based dispatch improves the total number of voltage violations again by nearly 100%. The time spent by the feeder in violation is improved by 99.4% at the cost of 2.46% of the total energy that could have been produced by the PV over the year. However, as indicated by the red line in Figure 47, there is even more disparity between the PV system curtailments over the year. The yearly distribution has a standard deviation of 9.78%. This result is at odds with the trends seen in previous control types and warrants further investigation. The distribution of relative curtailments throughout the circuit map for the worst week is shown in Figure 48. The PV systems curtailing the most are in the same area here as in Figure 26 for the Volt/Watt case, but localized directly around the capacitor, as shown in Figure 49. In fact, where under the local control all PV systems in this branch curtailed significantly more than the rest of the circuit, with the sensitivity-based control only a few PV system locations must curtail to improve the voltage of the whole branch.

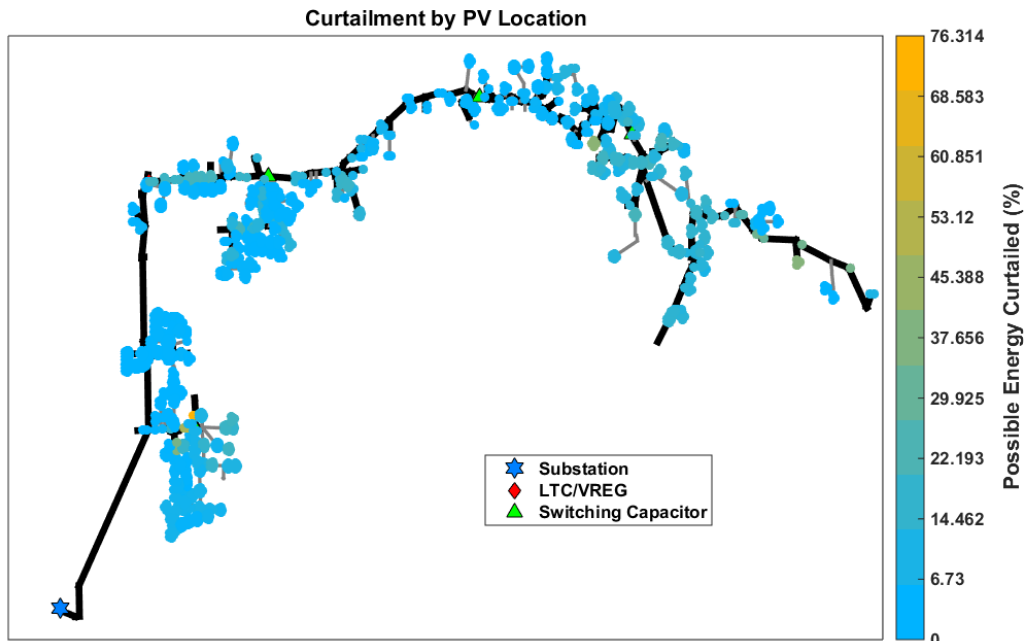


Figure 48. Geographic distribution of PV curtailments in the circuit due to sensitivity-based dispatch control during the worst week.

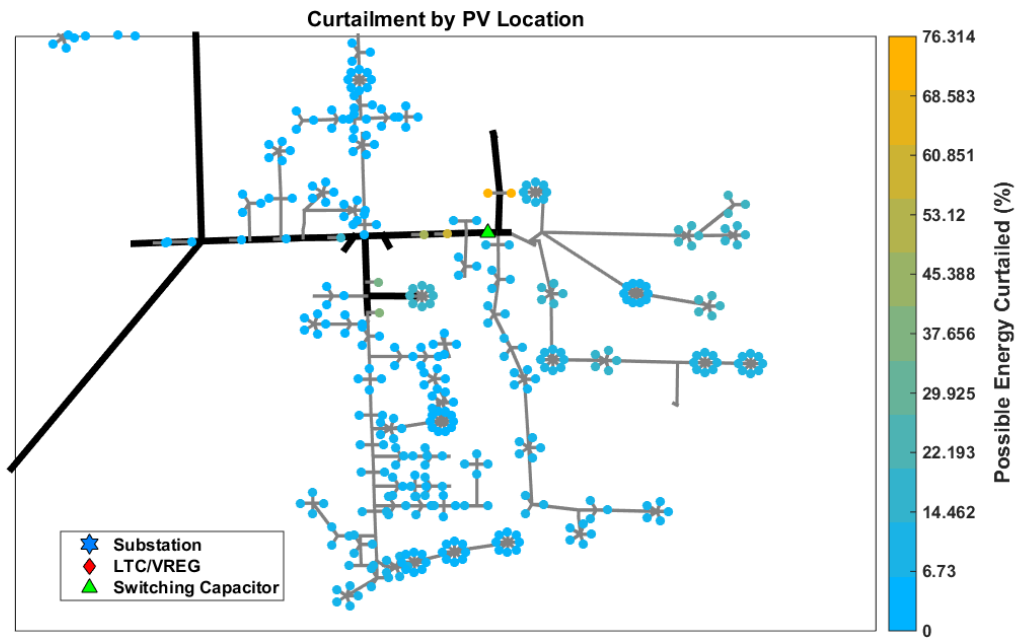


Figure 49. Zoomed-in section showing location of PVs curtailment the most due to sensitivity-based dispatch control during the worst week.

To see the difference in the control over the course of the year, the same relative PV system curtailments are plotted in Figure 50 using the full year results. The same small group of buses around the capacitor shown in Figure 49 curtail relatively more, yet there are also two other areas of the circuit that show large curtailment. The highest curtailment is now a cluster of PV systems that is towards the end of the feeder, but not near any obvious locations that would mitigate voltage rise. This is an interesting result of the sensitivity-based approach because it just so

happens that this is a relatively large cluster of PV systems that is well-positioned to improve the voltage profile of the end of the feeder. Therefore it is called on more by the sensitivity matrix to curtail to improve the overall feeder voltage. The other area that shows a higher level of relative curtailment over the year than during the worst week is just downstream of the voltage regulator. This section of the feeder is enlarged in Figure 51. Here it is clear the PV systems on the feeder backbone directly downstream of the voltage regulator are activated more by the control. This is most likely due to interactions between the inverters, the control, and the voltage regulator that occur at some points in the year that were not represented during the worst week of over-voltages from the base case.

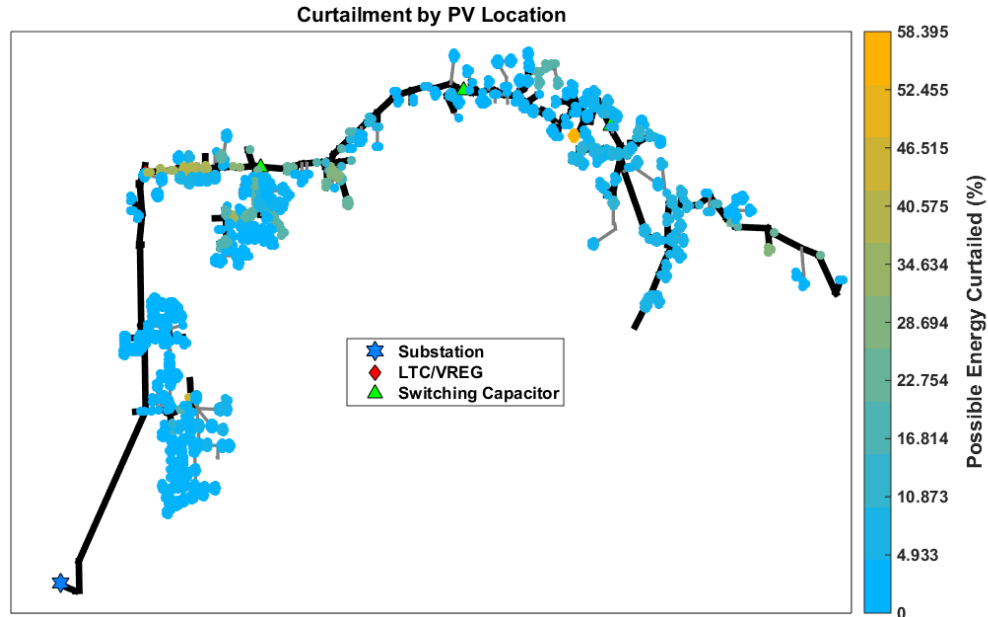


Figure 50. Geographic distribution of PV curtailments in the circuit due to sensitivity-based dispatch control over the year.

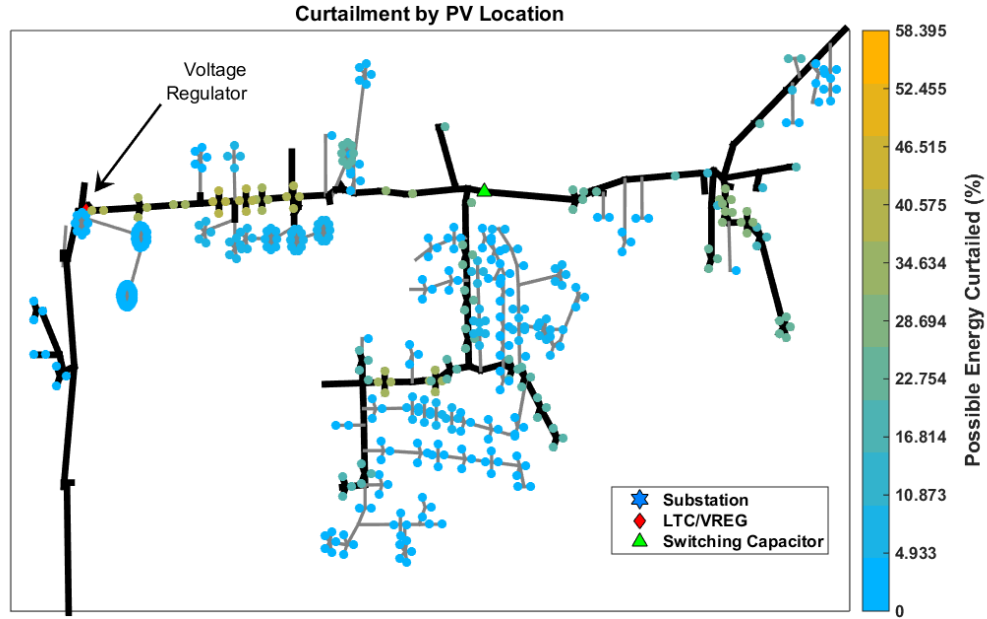


Figure 51. Zoomed-in section showing location of PVs curtailing more due to sensitivity-based dispatch control over the year than during worst week.

Five-minute Dispatch

The sensitivity-based control is tuned again under the assumption that the centralized controller can only dispatch signals once every five minutes to all the PV. Since it is assumed a larger dispatch window will require a slower controller to prevent oscillation, new parameter sets are selected to try. Sets #1-5 have $K_A = 0.9$ and $\Delta P_{lim} = [0.1, 0.2, \dots, 0.5]$, Sets #6-15 have $K_A = 1.0$ and $\Delta P_{lim} = [0.1, 0.2, \dots, 1.0]$, and Sets #16-20 have $K_A = 1.1$ and $\Delta P_{lim} = [0.1, 0.2, \dots, 0.5]$. A comparison in the performance of these control parameters is shown in Figure 52. In this instance, it is fairly clear that Set #1 minimizes both voltage violations, power curtailment, and is the least likely to result in oscillations due to its low ΔP_{lim} .

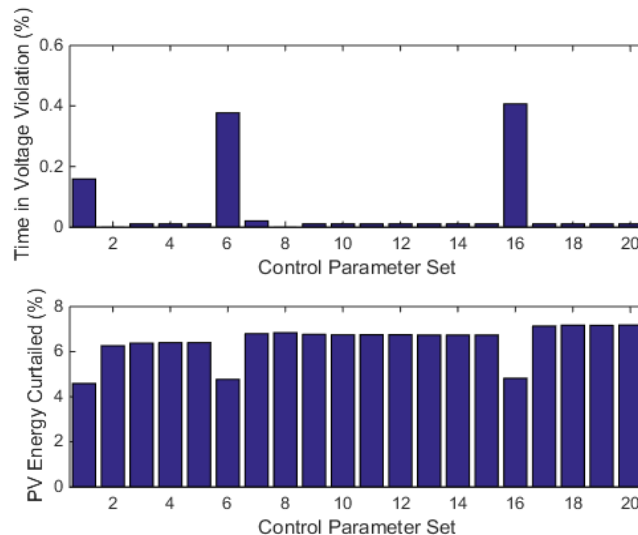


Figure 52. Comparison of sensitivity-based five-minute dispatch control parameter set performance.

Using $K_A = 0.9$ and $\Delta P_{lim} = 0.1$, the curtailment profile and remaining instances of over-voltage violations are shown in Figure 53. Overall, the controller performed similar to the one-minute dispatch. The overall voltage violations are reduced by 99.8% and the time spent in violation by the feeder is reduced by 98.9%. The PV systems were curtailed 4.58% of their total output.

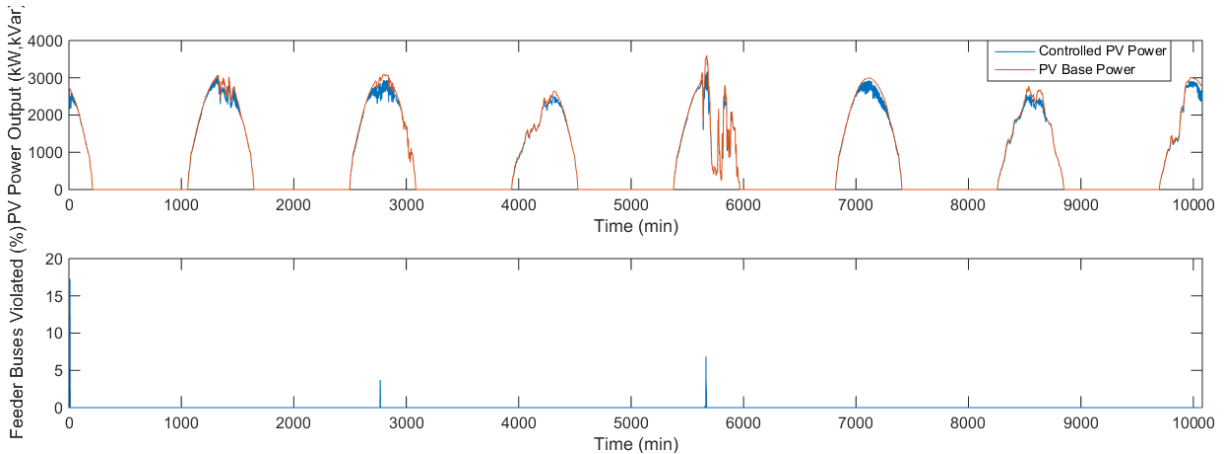


Figure 53. PV output power with and without five-minute dispatch sensitivity-based curtailment and remaining voltage violations with control.

However, there are a few major differences between the five-minute dispatch and the one-minute dispatch. The first is the presence of controller oscillations, which are noticeable by the “thick” blue power outputs in Figure 53. Zooming in on a single day in Figure 54, it is clear that these oscillatory power outputs are indeed the result of controller ringing as the controller is clearly saturating at the ΔP_{lim} value in an attempt to regulate the voltage. The five-minute dispatch is simply too slow to keep up with the changes of the system.

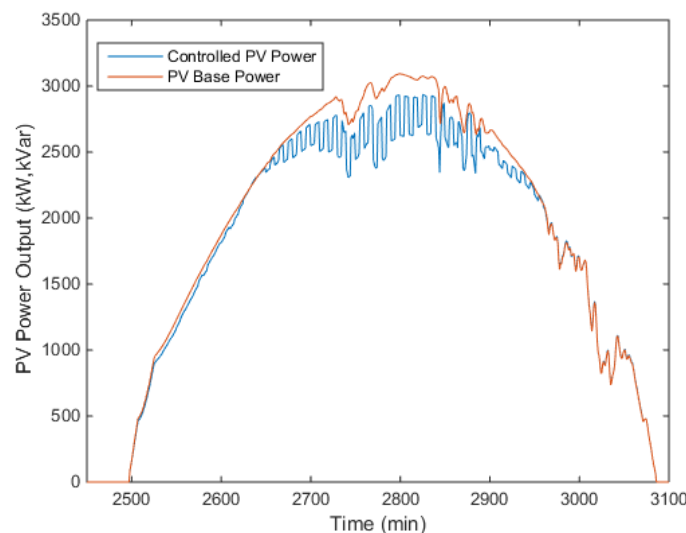


Figure 54. Zoomed-in section of a day under five-minute dispatch of sensitivity-based curtailment.

The second major difference is a peculiarity seen in the distribution of PV system curtailments in Figure 55. While the overall shape is similar to that of the 1-minute sensitivity-based dispatch,

the presence of negative “curtailment” values is disturbing. This means that several PV have actually produced more power under this control than in the base case, which is supposed to be the PVs’ maximum power output. At face value this appears to be an error in the control. However, the maximum increase is very small at 1.00% and may be the result of two things. First, the rating of each PV inverter was increased by 1% between the baseline run and this control to accommodate reactive power support. Second, each inverter has a cut-in and cut-out value that turns the inverter off if the PV system is not outputting above 10% of its rating, which is common in practice since inverters have poor efficiency at low power output. The result is that at least twice a day during the week, if no curtailment signal is applied, these PV systems will output slightly more than the baseline case. In effect, the result is negligible and any negative values should be considered practically zero. Overall there is a standard deviation of 8.23% in the distribution of power curtailment among all PV systems.

Simulating the full year of data with the sensitivity-based control using a 5-minute dispatch has a slightly worse improvement in over-voltage violations. Total over-voltages are reduced by 99.8% and time spent in violation is reduced by 99.2%. This is to be expected from the results of the fair dispatch and it makes sense since the control has fewer actions available to improve the voltage. The amount of energy curtailed is also slightly worse at 2.82%. The disparity in control action is shown as the red line in Figure 55 and has a standard deviation of 9.89%, also slightly worse than the 1-minute dispatch case. As with the 1-minute dispatch case, the one-year results have a higher disparity, mainly due to the interaction with some inverters and the voltage regulator.

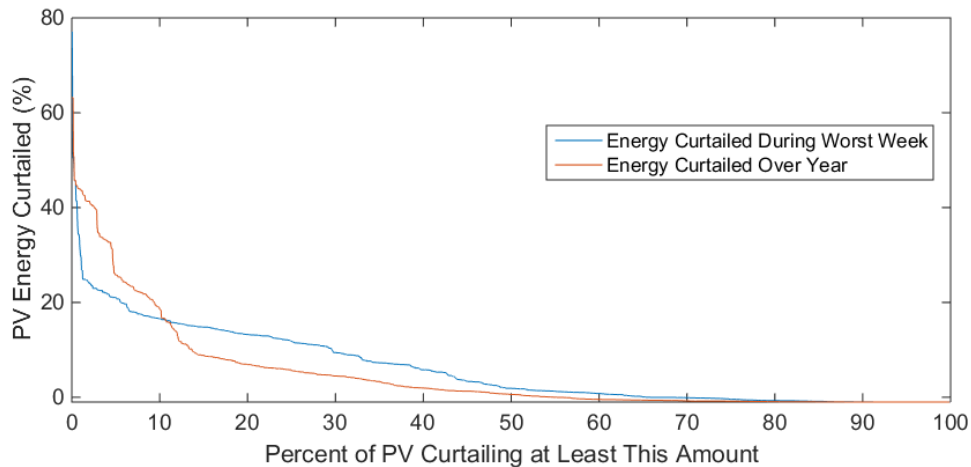


Figure 55. Disparity in PV power curtailment using sensitivity-based control dispatched at 5-minute intervals.

5. CONCLUSIONS

Below in Table 1 is a comparison of the different controls presented in Section 3 and how they performed during the worst one-week period of voltage violations during the year. The first row of each table compares how each control improves the overall sum of over-voltages at each bus and point in time. The second row compares how each control improves the time in which the feeder spends with an over-voltage violation present at *any* bus.

Table 1. Comparison of the performance of the various PV inverter control types investigated during the worst one-week period of voltage violations on the feeder.

Control Type	ZCI	Volt/ Watt	Volt/ Var	Central Fair (1m)	Central Fair (5m)	Sensitivity- based (1m)	Sensitivity- based (5m)
Overall Voltage Issues Mitigated (%)	100.0	100.0	98.7	100.0	91.7	100.0	99.7
Time with Violations Mitigated (%)	100.0	100.0	97.9	99.2	41.9	99.6	98.9
Power Curtailed (%)	21.6	4.35	0	9.3	5.89	3.99	4.58
Curtailment Deviation (%)	0.75	5.69	0	0.57	0.16	8.21	8.23

Subsequently, the comparison of how each control performed over the entire year is presented below in Table 2.

Table 2. Comparison of the performance of the various PV inverter control types investigated during over full year of load and irradiance data.

Control Type	ZCI	Volt/ Watt	Volt/ Var	Central Fair (1m)	Central Fair (5m)	Sensitivity- based (1m)	Sensitivity- based (5m)
Overall Voltage Issues Mitigated (%)	100.0	100.0	98.2	100.0	97.6	100.0	99.8
Time with Violations Mitigated (%)	100.0	100.0	96.7	99.3	88.4	99.4	99.2
Power Curtailed (%)	10.7	0.85	0	1.75	2.00	2.46	2.82
Curtailment Deviation (%)	0.46	1.81	0	0.09	0.05	9.78	9.89

The Volt/Watt control did as comparable a job of mitigating over-voltage violations as the simple method of preventing reverse current injection into the feeder through curtailment (zero current injection). Impressively, it achieved this while curtailing 94.8% less energy than the zero current injection method. Additionally, the application of Volt/Var control was able to mitigate

most voltage violations with no curtailment at all. The combination of Volt/Var control with curtailing the PV systems only when necessary should be able to prevent 100% of voltage violations at a minimal level of PV real power curtailment.

Compared with the local controls, the centralized control types had global network knowledge that allowed them to achieve specialized tasks. Specifically, the fair dispatch was able to prevent a large number of over-voltage violations while evenly distributing the burden of curtailment relative to the size of each PV system. Where the fair dispatch method was able to mitigate a large overall number of over-voltages at a small curtailment, it did a poor job of improving the overall time spent by the feeder in a violated state. Reducing the voltage limit setting in (1) should improve its violation mitigation performance but curtail more energy. Contrarily, the centralized control method that made use of the knowledge of each PV system's impact on the overall network voltage was able to mitigate essentially all over-voltage violations using the least amount of curtailment during the time it was tuned to improve. However, when applied to the full year of data, the sensitivity-based method began to poorly interact with the feeder's voltage regulator and actually curtail more power than both the fair approach and the local Volt/Watt approach (although the fair approach did not meet the objective of mitigating all violations). This result is unexpected and emphasizes that this control in particular, and possible others, should take more system measurements into consideration than just over-voltages to make sure the parameters selected do not have adverse effects on the existing voltage controls. Overall, the controls with the larger dispatch windows had poorer results, although not by much. Where the longer dispatch times really suffered was the introduction of power oscillations to the feeder, which was an adverse impact but could not be easily quantified. As with the local control, the centralized dispatch methods could also benefit from reactive power support, either in the form of a direct dispatch or a supporting local control at each PV system. Further research should be conducted on each control type to identify which pairs best with reactive power support.

To conclude, this paper compared the effectiveness of several advanced inverter controls on a large number of PV systems uniformly distributed in a realistic distribution feeder model. A year of one-minute resolution irradiance and load data was simulated, with the irradiance data spatially dispersed to simulate the effect of moving clouds. Inverter controls were then implemented to adjust the desired PV system real and reactive power outputs in an effort to mitigate over-voltage violations. The controls were compared on their effectiveness in mitigating over-voltage violations at the cost of curtailing real power or producing vars. The fairness of how the controls were distributed to the inverters was also studied. The local Volt/Watt control was able to prevent voltage violations while still allowing for reverse power flow without the need for a communication network. The local Volt/Var control was also able to prevent most over-voltage violations without curtailment. Combining the two controls should prevent all over-voltages with minimum curtailment without communication. However, both of these controls were based on their location in the circuit and were therefore not fair to all PV systems. Introducing a communication network allowed for specific objectives to be achieved, namely for the control to be as fair as possible or to use the least amount of power control. However, the parameter selection process for each of the controls did not scale from the subset of time to the full year. Tuning the control based solely on one set of over-voltage measurements did not take existing controls into consideration and therefore the controls could not be guaranteed to perform equally well at all other times. To better select control parameters, they should be tuned over the

entire time period in question or more metrics that influence the presence of over-voltages should be included in the tuning procedure, such as capacitor switching or regulator tap switches. Additionally, oscillations between inverter controls was observed but not penalized. Future research into the application of large numbers of inverter controls should have network stability as a first priority ahead of power quality and renewable energy production. However, the study of network stability may require additional data or more time-consuming simulation.

6. REFERENCES

- [1] M. J. Reno, K. Coogan, S. Grijalva, R. J. Broderick, and J. E. Quiroz, "PV interconnection risk analysis through distribution system impact signatures and feeder zones," in *IEEE PES General Meeting Conference & Exposition*, 2014, pp. 1-5.
- [2] S. S. Sena, J. E. Quiroz, R. J. Broderick, "Analysis of 100 SGIP Interconnection Studies," Sandia National Laboratories SAND2014-4753, 2014.
- [3] M. E. Baran, H. Hooshyar, S. Zhan, and A. Huang, "Accommodating High PV Penetration on Distribution Feeders," *IEEE Transactions on Smart Grid*, vol. 3, pp. 1039-1046, 2012.
- [4] M. Rylander, J. Smith, "Stochastic Analysis to Determine Feeder Hosting Capacity for Distributed Solar PV," EPRI Technical Report 1026640, 2012.
- [5] "Electric Rule No. 21: Generating Facility Interconnections," ed, January 2015.
- [6] J. W. Smith, W. Sunderman, R. Dugan, and B. Seal, "Smart inverter volt/var control functions for high penetration of PV on distribution systems," presented at the IEEE/PES Power Systems Conference and Exposition (PSC&E), Phoenix, AZ, 2011.
- [7] K. Turitsyn, P. Sulc, S. Backhaus, and M. Chertkov, "Local Control of Reactive Power by Distributed Photovoltaic Generators," presented at the IEEE Smart Grid Communications (SmartGridComm), Gaithersburg, MD, 2010.
- [8] M. J. Reno, R. J. Broderick, S. Grijalva, "Smart Inverter Capabilities for Mitigating Over-Voltage on Distribution Systems with High Penetrations of PV," presented at the IEEE Photovoltaic Specialists Conference (PVSC), 2013.
- [9] J. Seuss, M. J. Reno, R. J. Broderick, and S. Grijalva, "Improving distribution network PV hosting capacity via smart inverter reactive power support," in *IEEE Power & Energy Society General Meeting*, 2015, pp. 1-5.
- [10] K. Turitsyn, P. Sulc, S. Backhaus, and M. Chertkov, "Options for Control of Reactive Power by Distributed Photovoltaic Generators," *Proceedings of the IEEE*, vol. 99, pp. 1063-1073, 2011.
- [11] X. Huanhai, Z. Meidan, J. Seuss, W. Zhen, and G. Deqiang, "A Real-Time Power Allocation Algorithm and its Communication Optimization for Geographically Dispersed Energy Storage Systems," *IEEE Transactions on Power Systems*, vol. 28, pp. 4732-4741, 2013.
- [12] M. Farivar, C. R. Clarke, S. H. Low, and K. M. Chandy, "Inverter VAR Control for Distribution Systems with Renewables," presented at the Smart Grid Communications (SmartGridComm), 2011.
- [13] R. A. Jabr, "Minimum loss operation of distribution networks with photovoltaic generation," *IET Renewable Power Generation*, vol. 8, pp. 33-44, 2014.
- [14] A. Bonfiglio, M. Brignone, F. Delfino, and R. Procopio, "Optimal Control and Operation of Grid-Connected Photovoltaic Production Units for Voltage Support in Medium-Voltage Networks," *IEEE Transactions on Sustainable Energy*, vol. 5, pp. 254-263, 2014.
- [15] M. Farivar, R. Neal, C. Clarke, and S. Low, "Optimal inverter VAR control in distribution systems with high PV penetration," presented at the 2012 IEEE Power and Energy Society General Meeting, San Diego, CA, 2012.

- [16] X. Su and P. Wolfs, "Comprehensive Optimization of PV Inverter Reactive and Real Power Flows in Unbalanced Four Wire LV Distribution Network Operations," presented at the IEEE Power and Energy Society General Meeting, Vancouver, BC, 2013.
- [17] E. Dall'Anese, S. V. Dhople, and G. B. Giannakis, "Optimal Dispatch of Photovoltaic Inverters in Residential Distribution Systems," *IEEE Transactions on Sustainable Energy*, vol. 5, pp. 487-497, 2014.
- [18] Y. P. Agalgaonkar, B. C. Pal, and R. A. Jabr, "Distribution Voltage Control Considering the Impact of PV Generation on Tap Changers and Autonomous Regulators," *IEEE Transactions on Power Systems*, vol. 29, pp. 182-192, 2014.
- [19] Y. P. Agalgaonkar, B. C. Pal, and R. A. Jabr, "Stochastic Distribution System Operation Considering Voltage Regulation Risks in the Presence of PV Generation," *IEEE Transactions on Sustainable Energy*, vol. 6, pp. 1315-1324, 2015.
- [20] S. R. Abate, T. E. McDermott, M. Rylander, and J. Smith, "Smart inverter settings for improving distribution feeder performance," in *IEEE Power & Energy Society General Meeting*, 2015, pp. 1-5.
- [21] M. J. Reno and K. Coogan, "Grid Integrated Distributed PV (GridPV)," Sandia National Laboratories, SAND2013-6733, 2013.
- [22] M. J. Reno and K. Coogan, "Grid Integrated Distributed PV (GridPV) Version 2," Sandia National Laboratories, SAND2014-20141, 2014.
- [23] J. E. Quiroz, M. J. Reno, and R. J. Broderick, "PV-Induced Low Voltage and Mitigation Options," IEEE Photovoltaic Specialists Conference, New Orleans, LA, 2015.

DISTRIBUTION

1	MS1033	Robert J. Broderick	6112
1	MS1033	Abraham Ellis	6112
1	MS1140	Matthew J. Reno	6113
1	MS1140	Ross Guttromson	6113
1	MS0899	Technical Library	9536 (electronic copy)



Sandia National Laboratories